APPLICATION OF THE HYDRAULIC ANALOGY TO STUDY THE PERFORMANCE OF THREE AIRFOILS AT SUBSONIC AND SUPERSONIC SPEEDS

A THESIS

Presented to

The Faculty of the Division of Graduate Studies

Georgia Institute of Technology

In Partial Fulfillment

of the Requirements for the Degree

Master of Science in Aeronautical Engineering

by

Dallas Marlin Ryle, Jr.

July 1950

APPLICATION OF THE HYDRAULIC ANALOGY TO STUDY THE PERFORMANCE OF THREE AIRFOILS AT SUBSONIC AND SUPERSONIC SPEEDS

Approved:

Date Approved by Chairman July 14, 1950

ACKNOWLEDGEMENTS

The author wishes to express his sincere appreciation to Mr. H. W. S. LaVier for his suggestion of this topic and his generous and valuable help in its execution. He also owes a debt of gratitude to the reading committee, composed of Mr. H. W. S. LaVier, Mr. J. J. Harper, and Mr. H. R. Henry; and other members of the staff of the Daniel Guggenheim School of Aeronautics for their advice and suggestions.

The efforts of the shop personnel were most helpful in the formation of the models and construction of needed equipment and are sincerely appreciated.

TABLE OF CONTENTS

LIST OF TABLES

LIST OF FIGURES

LIST OF FIGURES (Cont.)

LIST OF FIGURES (Cont.)

APPLICATION OF THE HYDRAULIC ANALOGY TO STUDY THE PERFORMANCE OF THREE AIRFOILS AT SUBSONIC AND SUPERSONIC SPEEDS

SUMMARY

Two British airfoil profiles were tested in the Georgia Institute of Technology twenty foot by four foot Water Channel at subsonic and supersonic speeds over a range of angles of attack. A third profile, the Italian G. U. 4, was tested at the same supersonic speed and angles of attack previously used in a water channel examination of the G. U. 4 airfoil. The chord was increased by a hundred per cent in this investigation in order to study the effect of Reynolds Number. The water depth distributions for the three profiles were obtained by the probe method. Through application of the hydraulic analogy, pressure distributions were obtained from the water depth distributions, and lift, drag, and moment coefficients were in turn obtained from the pressure distributions by integration. These airfoil aerodynamic characteristics were compared to wind tunnel and theoretical results for the three profiles in air.

INTRODUCTION

Theoretical work on the analogy between flow of water with a free surface and compressible gas flow was first presented by Riabouchinsky[1] in 1932. Since that time, further extensions of this theory and practical applications have been made by such leaders in the field as Ernst Preiswerk,[2] Binnie and Hooker in England,[3] the National Advisory Committee for Aeronautics,[4] and North American Aviation Incorporated.[5] Preiswerk's proof and explanations of the application of gas dynamics methods to the flow of water with a free surface are probably the foremost in the field. He conclusively proved the validity of the hydraulic analogy as it stands today.

North American Aviation and the National Advisory Committee for Aeronautics were leaders in experimental applications of the

---

1 D. Riabouchinsky, Mechanique des fluides. Comptes Rendus, 195, 1932, pp. 998-999.

2 Ernst Preiswerk, "Application of the Methods of Gas Dynamics to Water Flows with a Free Surface".
Part 1. "Flows with No Energy Dissipation". NACA TM No. 934, 1940.
Part 2. "Flows with Momentum Discontinuities." NACA TM No. 935, 1940.

3 A. M. Binnie, and S. G. Hooker, "The Flow Under Gravity of an Incompressible and Inviscid Fluid Through a Constriction in a Horizontal Channel", Proceedings of the Royal Society. Vol. 159 (London, England) 1937. pp. 592-608.

4 James Orlin, Norman J. Linder, and Jack G. Bitterly, "Application of the Analogy Between Watern Flow with a Free Surface and Two-Dimensional Compressible Gas Flow". NACA TN No. 1185, 1947.
Arthur Kantrowitz, "The Formation and Stability of Normal Shock Waves in Channel Flows". NACA TN No. 1225, 1947.

5 J. R. Bruman, "Application of the Water Channel-Compressible Gas Analogy". North American Aviation Incorporated, Engineering Report NA-47-87, 1947.

hydraulic analogy. Their work indicated that with the proper equipment and methods, accurate quantitative as well as qualitative results could be expected from water channel experiments. These theoretical and experimental developments have led to a very convenient and quite satisfactory means for conducting aerodynamic investigations. This method is particularly useful in compressible gas study when no supersonic or high speed wind tunnels are available.

Work with the analogy at the Daniel Guggenheim School of Aeronautics was commenced by John Hatch in 1948.[6] He constructed a water channel for the purpose of making investigations relative to high speed aerodynamics, and carried out some preliminary tests with the equipment which demonstrated the considerable possibilities pointed out in previous work. Further testing, with some alteration of equipment, was undertaken by John Catchpole in 1949.[7]

Some of the advantages obtained through application of the hydraulic analogy and use of the water channel may be summarized as follows:

(1) The relative cost is low compared with wind tunnel or flight tests.

(2) Visual observations for the purposes of research or instruction of such phenomena as shock wave formation, vortices,

---

[6] John E. Hatch, "The Application of the Hydraulic Analogies to Problems of Two-Dimensional Compressible Gas Flow". Unpublished Master's thesis, Georgia Institute of Technology, Atlanta, 1949.

[7] Eric John Catchpole, "Application of the Hydraulic Analogy to Study the Performance of two Airfoils in Compressible Flow". Unpublished Master's thesis, Georgia Institute of Technology, Atlanta, 1949.

turbulence, and flow pattern are possible. These same characteristics may also be photographed.

(3) High supersonic Mach numbers are obtained at model speeds of a few feet per minute.

(4) Any Mach number may be achieved by a simple speed setting while a nozzle change is required in wind tunnel work.

(5) Since no choking can occur, transonic observations are just as simple as for subsonic and supersonic speeds in the movable model type of water channel.

The present investigation is largeley concerned with (5) above, since most ofthe tests were conducted at Mach numbers close to unity. Supersonic and subsonic test results have proved the water channel experimental values to be reliable. By virtue of this fact, it is expected than the transonic water channel results will also be reliable. In partial fulfillment of these requirements, two of the three models used were tested in the transonic range in the Georgia Tech Water Channel. Much more than necessary attention was paid to the accuracy of water channel results and procedures for application to air flow as compared with other experimental and theoretical results and procedures.

LIST OF SYMBOLS

a - Speed of sound in gas

C_D - Section drag coefficient

C_L - Section lift coefficient

C_M - Section moment coefficient, referred to leading edge

$C_{M_{\frac{1}{4}}}$ - Section moment coefficient, referred to quarter chord

C_P - Local pressure coefficient

c_p - Specific heat of gas at constant pressure

c_v - Specific heat of gas at constant volume

γ - Adiabatic gas constant, ratio of c_p to c_v

d - Water depth

F_c - Compressibility Factor

$^{\circ}F$ - Degrees Fahrenheit

g - Acceleration due to gravity

h - Enthalpy

M - Mach number

p - Pressure of gas

ρ - Density of gas

R - Reynolds number

T - Absolute temperature of gas

V - Velocity of flow

ϕ - Velocity potential in two-dimensional flow

α - Angle of attack

x, y - Rectangular coordinates in the flow plane

u, v - Components of flow velocity in x and y directions, respectively

LIST OF SYMBOLS (Cont.)

Subscripts

No subscript - Any value of variable

l - Local value of variable

o - Value at stagnation

s - Value in undisturbed stream

max - Maximum value of variable

x - Partial derivative with respect to x

e.g. $\phi_x \equiv \frac{\partial \phi}{\partial x}$, $\phi_{xx} \equiv \frac{\partial^2 \phi}{\partial x^2}$

y - Partial derivative with respect to y

THEORY

The theory of the hydraulic analogy as presented by Ernst Preiswerk[8] will be reviewed here.

This theory of the analogy between water flow with a free surface and two-dimensional compressible gas flow depends on the following assumptions:

(1) The flow is irrotational.

(2) The vertical acceleration of the water is negligible compared with the acceleration due to gravity so that pressures in the fluid depend only on the heighth of the free surface above the point in question.

(3) There are no viscous losses, thus excluding the conversion of energy into heat or internal energy.

The energy equations for water and for gas give the relations shown below in terms of velocity.

For water this equation gives

$$v^2 = 2g(d_o - d)$$

$$V_{max} = \sqrt{2g\, d_o}$$

and for gas

$$v^2 = 2g\, c_p (T_o - T)$$

$$V_{max} = \sqrt{2g\, c_p\, T_o}$$

It can be seen that V/V_{max} for water and air are equal if

$$\frac{T_o - T}{T} = \frac{d_o - d}{d_o}$$

or, if

$$\frac{d}{d_o} = \frac{T}{T_o}. \qquad (1)$$

---

[8] Ernst Preiswerk, op. cit.

This comparison of water depth ratio, d/d_o, to the gas temperature ratio T/T_o, in the consideration of velocity is the first step in the proof of the analogy.

The equations of continuity are now compared. For steady two-dimensional gas flow, this equation is

$$\frac{\partial(u\rho)}{\partial x} + \frac{\partial(v\rho)}{\partial y} = 0$$

and for water

$$\frac{\partial(ud)}{\partial x} + \frac{\partial(vd)}{\partial y} = 0.$$

From these equations, a further step in the analogy is evolved as

$$\frac{d}{d_o} = \rho/\rho_o \quad (2)$$

By comparing equations (1) and (2), it is seen that the analogy holds only if the following equation is satisfied by the gas in question.

$$\frac{T}{T_o} = \rho/\rho_o \quad (3)$$

However, the temperature and pressure of the gas must also conform to the principles of the adiabatic relation (assumption (3))

$$\left(\frac{T}{T_o}\right)^{\frac{1}{\gamma-1}} = \rho/\rho_o \quad (4)$$

An inspection of equations (3) and (4) reveals that they are simultaneously only if $\gamma = 2$.

Thus, the flow of water is analogous to the flow of a gas having $\gamma = 2$. Since γ for air is 1.4, this appears to be a rather loose

comparison. However, many characteristics of gas flow do not depend strongly on γ . The significance of this statement will be further illustrated.

Consider now the adiabatic relation and the preceding numbered equations,

$$\frac{p}{p_o} = \left(\rho/\rho_o\right)^{\gamma} = \left(\rho/\rho_o\right)^{2}$$

or

$$\frac{p}{p_o} = \left(\frac{d}{d_o}\right)^{2} \qquad (5)$$

The differential equation of the velocity potential for water is as follows:

$$\Phi_{xx}\left(1-\frac{\Phi_x^2}{gd}\right)+\Phi_{yy}\left(1-\frac{\Phi_y^2}{gd}\right)-2\,\Phi_{xy}\,\frac{\Phi_x\,\Phi_y}{gd}=0 \qquad (6)$$

and the corresponding equation for gas is

$$\Phi_{xx}\left(1-\frac{\Phi_x^2}{a^2}\right)+\Phi_{yy}\left(1-\frac{\Phi_y^2}{a^2}\right)-2\,\Phi_{xy}\,\frac{\Phi_x\,\Phi_y}{a^2}=0. \qquad (7)$$

Equations (6) and (7) are identical if

$$\frac{gd}{2gd_o} = \frac{a^2}{2gh_o}$$

From this relation it is seen that $\sqrt{gd}$ corresponds to the pressure propagation velocity or velocity of sound, a, in gas flow. The expression $\sqrt{gd}$ is the basic wave propagation velocity in shallow water with a free surface as proved by Leigh Page.[9]

---

[9] Leigh Page, Introduction to Theoretical Physics. D. Van Nostrand Co., Inc., 1928, pp. 218-224.

In water flowing at speeds above $\sqrt{gd}$, the velocity of the flow may strongly decrease for short distances and the depth may increase. An unsteady motion of this type is called a hydraulic jump, and corresponds to a shock wave in a gas.

This completes the analogy which is summarized in the following table of corresponding quantities and characteristics.

Two-Dimensional Compressible Gas Flow, $\gamma = 2$	Analogous Liquid Flow
Temperature ratio, T/T_o	Water-depth ratio, d/d_o
Density ratio, ρ/ρ_o	Water-depth ratio, d/d_o
Pressure ratio, p/p_o	Square of water-depth ratio, $(d/d_o)^2$
Velocity of sound, $a = \sqrt{\frac{\gamma p}{\rho}}$	Wave velocity, $\sqrt{gd}$
Mach number, V/a	Mach number, $V/\sqrt{gd}$
Shock wave	Hydraulic jump

The application of the analogy as it will be used in this investigation is as follows:

The Mach number of the free stream may be calculated as

$$M_s = \frac{V_s}{\sqrt{g d_s}} \qquad (8)$$

The standard equation for the pressure coefficient at any point on an airfoil is defined in the supersonic case as

$$C_p = \frac{p_l - p_s}{\frac{1}{2}\rho_s V_s^2} \qquad (9)$$

and in the subsonic case[10] as

$$C_p = F_c \left[\frac{p_l/p_s - 1}{p_o/p_s - 1} \right]. \qquad (10)$$

Since

$$\frac{1}{2}\rho_s V_s^2 = \frac{1}{2}\rho_s a_s^2 M_s^2$$
$$= \frac{1}{2}\rho_s \left(\frac{\gamma p_s}{\rho_s}\right) M_s^2$$
$$= \frac{\gamma}{2} p_s M_s^2,$$

equation (9) simplifies to

$$C_p = \frac{2}{\gamma M_s^2} \left[p_l/p_s - 1 \right].$$

From equation (5)

$$\frac{p_l}{p_s} = \left(\frac{d_l}{d_s}\right)^2$$

Therefore, in the present consideration, γ=2.0, equations (9) and 10) evolve as

$$C_p = \frac{1}{M_s^2} \left[\left(\frac{d_l}{d_s}\right)^2 - 1 \right] \qquad (11)$$

and

$$C_p = F_c \left[\frac{\left(\frac{d_l}{d_s}\right)^2 - 1}{\left(\frac{d_o}{d_s}\right)^2 - 1} \right]. \qquad (12)$$

---

[10] James Orlin, Norman J. Linder, and Jack G. Bitterly, "Application of the Analogy Between Water Flow with a Free Surface and Two-Dimensional Compressible Gas Flow". NACA TM No. 1185, 1947.

The compressibility factor for a compressible gas is

$$F_c = \frac{2}{\gamma M_s^2}\left[\left(1 + \frac{\gamma-1}{2} M_s^2\right)^{\frac{\gamma}{\gamma-1}} - 1\right].$$

Since the hydraulic analogy requires that $\gamma = 2.0$, the compressibility factor simplifies to

$$F_c = 1 + \frac{1}{4} M_s^2 \qquad (13)$$

Thus, by virtue of the hydraulic analogy, applicable equations for the pressure coefficients from which all airfoil characteristics data is obtained are set forth.

EQUIPMENT

There are two types of water channels suitable for application of the hydraulic analogy. The least expensive of these two is the type in which the model is moved through static water. The other arrangement is one in which the model remains stationary while water flows past it. The former is in use at Georgia Tech and the Aerophysics Laboratory of North American Aviation, Incorporated[11] while the latter is employed by the National Advisory Committee for Aeronautics at Langley Field, Virginia.[12]

Other advantages of the movable model type include easy acceleration of the flow, simple construction, and no boundary layer effect from the sides and bottom of the channel. Its biggest disadvantage, which is not present in the stationary model arrangement, is the difficulty of measuring the water depth along the model.

A general view of the water channel is shown in Figure 1. The frame is of bolted structural steel supporting a channel four feet wide, twenty feet long, and approximately one and one fourth inches in depth. The bottom of this channel is of plate glass in two five foot sections and one ten foot section. The transverse steel members are spaced at thirty inch intervals and are supported by screw jacks enabling the glass surface over which the model slides to be leveled

---

[11] J. R. Bruman, op. cit.

[12] James Orlin, Norman G. Linder, and Jack G. Bitterly, op. cit.

within 0.001 inch at all points. This leveling is accomplished through use of a depth gage; this instrument is also used before each run to determine the static depth of the water in the test section within 0.0005 inch.

A drain is provided at one end of the channel.

The model carriage is of welded steel tubing construction. It is moved along the channel on four rubber wheels which transfer the weight of the carriage to the upper horizontal steel members of the frame, serving also as rails. Four rubber wheels with vertical axes located at the carriage frame corners prevent any relative sidewise motion of the carriage. The model is supported ahead of the carriage by a vertically free acting mount producing the towing force and permitting the model weight to act on the channel bottom. This mount is also radially adjustable and calibrated in order that the angles of attack can be measured accurately. Safety stops are placed at the ends of the carriage track to prevent overrunning of carriage and model.

The carriage is driven by a one-quarter horse-power, single phase, alternating current electric motor through a 3/32 inch continuous steel cable. A reversing mechanism and a "Speed-Ranger" device enable control of motion in either direction and at varied speeds. An auxiliary power unit is available for high speed and accelerating and decelerating runs. This consists of a 19.5 amp, 24 volt direct current series wound motor which drives the cable through a set of reduction gears.

The combination of these two drive units provides speeds of

from 0.5 to 5.5 feet per second. A photograph of the drive mechanism is shown in Figure 2.

The correct timing for accurate speed adjustment of the model is accomplished by means of a microswitch placed on the track. A cam 2.925 feet in length attached to the carriage trips this switch which automatically operates an electric timer. The timer is located on the control panel above the water channel. This panel also contains the instruments and switches for starting, reversing, and operating the drive mechanism.

When experimental work was first begun in the Georgia Tech Water Channel, photographs were taken of the models to determine the water depth distribution around the model. The method and equipment used in this work are described by Hatch.[13] Photographic interpretation of these results was not particularly accurate so another method of measuring water depth was developed.

The model is fitted with a plexiglas bracket from which are suspended steel needle probes alongside the upper or lower surface of the model at intervals of 0.1 chord and 0.1 inch out from the model surface. These probes are attached to adjustable brass screws which are screwed into brass bushings fitted into the plexiglas bracket. Copper contacts are provided for each probe. Contact of the probe with the water completes the grid circuit of a vacuum tube causing a relay to operate a signal light. As the model is moved through the water, the probe is adjusted vertically until it just touches the water. The status of the signal light determines the contact position

---

[13] Hatch, op. cit.

of the probe point and the water surface. This is done for each of the probes and the water depths are then measured by means of a heighth gage and surface plate to within an accuracy of 0.001 inch. A photograph of one of the models with the probes in place is presented in Figure 6.

Although no photographs were taken for the purpose of experimental data, Figure 7 was included to show the flow pattern from the bi-convex model in motion in the water channel.

The models were chosen because of the availability of both subsonic and supersonic wind tunnel data. The models and a brief description are as follows:

(1) Faired double wedge airfoil, 8.7 per cent thick.[14] The model was constructed of lacquered hard brass and had a 12 inch chord. A descriptive diagram is shown in Figure 3.

(2) Symmetrical bi-convex airfoil, 7.5 per cent thick.[15] This was also constructed of lacquered hard brass and had a 12 inch chord. A diagram is presented in Figure 4.

(3) Triangular G. U. 4 airfoil, 6.1 per cent thick.[16] The model was constructed of shelacked mahogany and had a 24 inch chord. This model is shown in Figure 5.

---

[14] W. F. Hilton and F. W. Pruden, "Subsonic and Supersonic High Speed Tunnel Tests of a Faired Double Wedge Aerofoil". BARC R&M No. 2057, 1943.

[15] W. F. Hilton, "Subsonic and Supersonic Tests on a 7.5 per cent. Bi-convex Aerofoil". BARC R&M No. 2196, 1944.

[16] Antonio Ferri, "Experimental Results with Airfoils Tested in the High Speed Tunnel at Guidonia". NACA TM No. 946, 1940.

PROCEDURE:

A test run was conducted for both the upper and lower surfaces of the model at each angle of attack and each Mach number. The carriage speed was adjusted in accordance with the Mach number, the static water level adjusted to the proper depth, and the desired angle of attack set before each of these test runs. The probes were adjusted during the tests by trial until they indicated the local depths alongside the model. These depths were measured and recorded for future use in calculating the pressure coefficients. The equipment used to accomplish these tests has been described in the previous section.

TESTS CONDUCTED:

The following tests were conducted at a static water depth of 0.250 inch under the conditions described below.

Faired Double Wedge Airfoil

$M = 1.45$ $\alpha = -5, -4, -2, 0, 2, 4$ degrees

$M = 1.21$ $\alpha = -5, -4, -2, 0, 2, 4, 5$ degrees

Bi-convex Airfoil

$M = 1.25$ $\alpha = -4, -2, 0, 2, 4,$ degrees

G. U. 4 Airfoil

$M = 2.13$ $\alpha = -2, 0, 2, 6$ degrees

The tests conducted at a static water depth of 0.750 inch were:

Faired Double Wedge Airfoil

$M = 0.80$ $\alpha = -2, 0, 4, 7$ degrees

Bi-convex Airfoil

$M = 0.80$ $\alpha = -4, -2, 0, 2, 4$ degrees

COMPARISON AND DISCUSSION

Each of the airfoils tested will be discussed separately which will involve some repetition but allow a more thorough coverage.

Faired Double Wedge Airfoil

This airfoil was tested as described in the previous section. A sample calculation for the pressure coefficient and also the corrected pressure coefficient is presented in Table I of Appendix I. All of the pressure coefficients as calculated by Equation 9, using $\gamma = 2.0$, were corrected to $\gamma = 1.4$ by means of a correction procedure deduced from Figure 1 of the National Advisory Committee for Aeronautics Technical Note 1185.[17] Results were obtained for both $\gamma = 1.4$ and 2.0 by integrating the plotted pressure distributions, examples of which are shown in Figures 8, 9, 10, and 11.

Values of lift, drag, and moment coefficients are shown in Table II and plotted in Figures 15, 16, 17, 18, 19, 20, 21, 22, and 23. These plots present both the corrected and uncorrected measured values in comparison with wind tunnel tests[18] and either the Busemann or extrapolated Ackeret theory when applicable.

Figures 8 and 10 represent the supersonic chordwise pressure distribution as being typical of the plots obtained for this airfoil. Figure 9 represents a typical supersonic thicknesswise pressure distribution and Figure 11 the subsonic chordwise pressure distribution.

---

17 James Orlin, Norman Linder, and Jack Bitterly. op. cit.

18 W. F. Hilton and F. W. Pruden. op. cit.

Since there is no means for direct comparison of these plots to either wind tunnel or theoretical results, only a general discussion can be presented.

Figure 10 shows a small unexpected pressure peak for the lower surface at approximately 0.30 chord. This may probably be attributed to a bow disturbance of approximately 2.5 inches width, centering at the leading edge, which invalidates assumption (2) of the theory concerning negligible vertical accelerations at that point. Discrepancies are also noticeable in approximately the same location in Figure 8. A similar sharp breaking peak occurs at about 0.75 chord for the upper surface in Figure 8 and is believed to have been caused by expansion waves aft of the point of maximum thickness. Although a positive increase is expected in the pressure coefficient close to the trailing edge, it is unlikely that it increases as rapidly as is evidenced in particular by the lower surface in Figure 8. It is very possible that a separation of the flow in this neighborhood occured which caused this increase. If that be the case, the pressure distribution will correspond more closely at the trailing edge to a wind tunnel plot than to a theoretical plot.

Figure 9 requires no particular discussion since a thickness pressure plot is not suitable for discussion as to trends and effects.

As is to be expected, the chordwise pressure distribution for Mach number of 0.8 is smoother in shape than for the supersonic plots. The negative pressure peaks occur at the approximate location of the points of reflex for the upper and lower surface, but the steep slope of the curves toward the trailing edge definitely indicates separation

of the flow. A positive peak also occurs at about 0.25 chord which is partially caused by the bow disturbance, again invalidating assumption (2) of the theory at this point.

A slight clockwise tilting of the water level about the half chord, more noticeable in the deeper water subsonic tests, produces a slight gradient error in the probe readings which produces larger pressure coefficients for the forward half of the chord and smaller coefficients for the aft half. It is believed by the writer and other observers that this gradient error is a function of local velocities and friction of the water on the model.

The corrected pressure coefficient curves seem to follow the $\gamma = 2.0$ coefficient curves with little deviation, but a closer scrutiny shows small differences which reveal themselves in the lift, drag, and moment results.

It is believed that there is a basic error of very small consequence in the equipment and procedure setup which will affect the pressure distribution slightly. This will be discussed in a later section.

A review of Figures 15 through 23 reveals that the water channel results follow the correct trends and with a few exceptions, the quantitative agreement with the theoretical and wind tunnel results is good. An occasional "wild" point such as the $\alpha = 0^{\circ}$ point of Figure 16, $\alpha = 2^{\circ}$ of Figure 19, and $\alpha = 4^{\circ}$ of Figure 23 is noted. Since the agreement is generally close, these points are apparently effects of human error and technological inconsistencies. Particularly good results are noted

for the lift comparisons with the greater deviations occuring at the larger angles of attack for all of the coefficient presentations.

It is seen that the γ correction is of notable importance since it corrects the experimental results in the right direction almost without exception. Although this correction is usually small, it is definitely a step in the right direction.

The corrected values approach the theoretical curves more closely than to the wind tunnel results which is in opposition to the findings of Catchpole's investigations.[19] However, agreement between analogous results and theoretical results is to be expected since neither theory nor water channel calculations include viscosity effects which do appear in wind tunnel test results.

Bi-Convex Airfoil

The tests and methods of calculating results are the same for this airfoil as for the faired double wedge airfoil. A summarization of the test coefficients is presented in Table III of Appendix I and the corresponding curves appear as Figures 25 through 29 where they are compared to wind tunnel results[20] and extrapolated Ackeret theory when applicable.

A typical thickness pressure distribution is shown for a Mach number of 1.25 in Figure 12. The effect of the γ correction is plainly evident in this case since the area over the lower surface is larger

---

19 John Catchpole. op. cit.

20 W. F. Hilton. op. cit.

in the case of $\gamma = 1.4$ than for $\gamma = 2.0$. The subsonic chordwise pressure distribution of Figure 13 is very similar to the subsonic pressure distribution for the faired double wedge airfoil with the same trensd at the leading and trailing edge. However, the decrease in pressure coefficient at the trailing edge is not as noticeable as in Figure 11.

Figures 24, 25, and 26 show that the water channel results follow the correct trends with very good quantitative agreement in the case of lift and moment. However, it is noted that the experimental results approach wind tunnel values more closely than to the theoretical curves. This may be coincidental since the wind tunnel and theoretical curves are also in relatively close agreement and there are several chances for error in obtaining the final experimental values. The γ correction seems to affect only the drag coefficients in any appreciable amount. It is believed that the close supersonic quantitative agreement, especially in the case of the moment coefficients which are difficult to obtain accurately, is a result of the small flow deflection angles for the model.

Figures 27, 28, and 29, which represent the subsonic investigations, reveal desirable qualitative agreement but the quantitative results are not as good as in the case of the supersonic comparisons. This may be explained by a previous assumption that there is a more active separation of flow close to the trailing edge at this high speed "streaming" condition. It has been a general observation that better results are obtained at the lower angles of attack. Since there would be a greater tendency for flow separation and other flow inconsistencies

to occur at the higher angles of attack, it would appear that this assumption of flow separation is valid.

G. U. 4 Airfoil

As was stated in a previous section, the main purpose of the experiments on this airfoil is a Reynolds Number consideration. Tests were conducted by Catchpole[21] on this same profile at the Mach number used in the present investigation. However, the chord was increased by 100 per cent to give a basis for Reynolds number comparison.

The test coefficients for this airfoil are compiled in Table IV of Appendix I and are depicted graphically in Figures 30, 31, and 32 as comparisons to Ferri's wind tunnel balance tests at Guidona[22] and calculations based on the "exact" theory.

The Reynolds number used in Ferri's wind tunnel tests at Guidonia was approximately 720,000 while Catchpole's tests were conducted at a Reynolds number of 203,000 calculated for a water temperature of 86°F. The investigations presented herein were made at twice the previously used number of 203,000 or 406,000. This approaches the Guidonia Reynolds number near enough for there to be only small discrepancies in results as far as Reynolds number effects are concerned.

A sample pressure coefficient plot is presented in Figure 14

---

21 John Catchpole. op. cit.

22 Antonio Ferri, "Experimental Results with Airfoils Tested in the High Speed Tunnel at Guidonia". NACA TM No. 946, 1940.

along with a theoretical pressure distribution for $\gamma = 1.4$ and $\gamma = 2.0$ using Busemann's parabolic formula.[23] A similar observation as to the effect of the bow disturbances on the pressure coefficient for the first portion of the airfoil is noted for this airfoil as for the faired double wedge profile. A slight increase of both the upper and lower surface pressure coefficients toward the trailing edge indicates the effect of flow separation. This effect is more pronounced at the higher angles of attack pressure distributions which aren't presented in this thesis. The lower surface coefficients are somewhat higher than expected and suggest a basic error in method.

Figures 30, 31, and 32 reveal the correct trends with fair quantitative agreement noticed for drag and moment and a better comparison for the lift coefficients. The tendency for the coefficients to approach theoretical results is even more noticeable for this profile than for the faired double wedge airfoil. This is particularly evident in Figure 31, where the test results depart from wind tunnel values considerably and follow the same path as Busemann's theory.

A comparison of the results obtained in this investigation with the Catchpole's results indicates an approximate average of 25 per cent closer quantitative agreement with theory and wind tunnel for the higher Reynolds number tests. However, all of the results obtained and presented in this investigation have been generally better than

---

23 E. Arthur Bonney, "Aerodynamic Characteristics of Rectangular Wings at Supersonic Speeds". Journal of the Aeronautical Sciences. Vol. 14: 1947, pp. 110-116

those of previous investigations due to improved methods of experimentation and study. Nevertheless, since this model was constructed of mahogany which is not as conducive to good flow conditions or as accurate in construction as a brass model, it is very likely that the higher Reynolds number effect was an aid in securing better results.

General Discussion

The results obtained in this investigation surpassed expectations as to both their quantitative and qualitative accuracy in agreement with theoretical and wind tunnel values. The trends are almost without exception correct and seem to adhere more closely to the paths followed by theory which, as has been previously explained neglects the effects of viscosity. The several new experimentation methods and techniques which have been incorporated since previous investigations are responsible for these improved test results.

The most consistent discrepancies in test coefficients occured in the drag considerations. This is easily explained in that an integration of the thickness wise pressure distribution for the determination of the drag coefficient is an approximation at best due to the nature of the points which fall in close proximity to each other in an inconsistent pattern. However, this method is sufficiently accurate to indicate general results.

The nature of Equation (11) of the theory section, $C_p = \frac{1}{M_s^2}\left[\left(\frac{d_1}{d_s}\right)^2 - 1\right]$, is such that it can be seen that a small error in the measurement of d_1, d_s, or M_s can produce a considerable error in C_p. Also, the

technique by which the γ correction for C_p is obtained possesses possibilities of error. However, the methods of measuring M_s, d_l, and d_s have been improved to the point where there should not be any errors of large consequence in C_p. Nor should the errors in the corrected C_p be great since it depends on the original $\gamma = 2.0$ C_p and values taken from Figure 1 of the National Advisory Committee for Aeronautics Technical Note 1185. In spite of these new and improved techniques, there is still the probability of small errors in the determination of the coefficient of pressure for both $\gamma = 2.0$ and 1.4, contributing to the fact that some of the water channel lift curve slopes presented here, with the slopes of the theoretical lift curves indicates an approximate 7 per cent average error with the largest discrepancy of 15 per cent occuring for the biconvex profile at a Mach number of 1.25. A similar comparison for the slopes of the moment curves reveals an error of approximately 15 per cent. A consideration of the agreement between the quantitative experimental and theoretical drag coefficients shows a very general average error of about 14 per cent.

Although Busemann's theory gives an approximate constant error in the change of γ from 1.4 to 2.0, the error in, for example, the lift coefficient for the G. U. 4 airfoil at $M = 2.13$ and 0° is approximately 30 per cent because of the small absolute value of the lift coefficient at this point. The percentage error drops to a much smaller value at the higher angles of attack where the absolute value of the lift coefficient is relatively large. The importance of the γ correction

for test results is evident since most supersonic flight work will be conducted at low angles of attack. A general resumé of the presented performance curves indicates that this first attempt at a correction has been succussful in that it has improved the qualitative trends of the curves somewhat and has been a particular improvement in quantitative results. The increments in coefficient values brought about by the change from $\gamma = 2.0$ to 1.4 are reasonably consistently of the same magnitude for any one curve as is expected since the increments calculated from Busemann's formula are approximately of the same value also.

A general failing of the hydraulic analogy is the fact that it only takes into account normal pressures in the determination of lift, drag, and moment coefficients, whereas shear effects are neglected. This factor contributes to the generally closer agreement between water channel test results and theoretical values than between water channel test results and wind tunnel data which, of course, takes into account viscosity effects.

The shortcomings of the hydraulic analogy and its application in the present investigation have been pointed out in this section along with a brief discussion of results. These shortcomings are now of relatively small consequence as a result of the improved methods and techniques employed. The results are a good indication of this but there is still room for further improvement and development.

CONCLUSIONS

As was stated in the Summary, an investigation of two British airfoils and a Guidonia airfoil was conducted through application of the hydraulic analogy. The performance results have been compared to wind tunnel and theoretical results and are presented herein.

There was a vast improvement in the quantitative agreement with the values used for comparison than in previous investigations as a result of improved experimental equipment and techniques. Good quantitative agreement was expected and was obtained since the hydraulic analogy has yielded the correct trends in past investigations by Hatch,[24] Thomas,[25] and Catchpole.[26] It was also roughly determined that there is an effect of Reynolds number on testing results; a high Reynolds number giving better results.

This application of the hydraulic analogy has been the first at Georgia Tech to employ a γ correction in the determination of C_p. The overall effect of this correction indicates that it should be used in future experiments as it produces a definite improvement in results.

The majority of the tests were conducted at high subsonic and low supersonic speeds. By virtue of this fact, it was a particular

---

[24] John Hatch. op. cit.

[25] Gerald B. Thomas, "Application of Water Channel Compressible Gas Analogies to Problems of Supersonic Wind Tunnel Design". Unpublished Master's Thesis, Georgia Institute of Technology, 1949.

[26] John Catchpole. op. cit.

pleasure to note the excellent results since transonic phenomena is very difficult to study in a wind tunnel.

Thus, the water channel has proven itself to be an inexpensive, easily operated, and very useful means of studying the problems of two dimensional compressible flow. Subsequent development of experimental techniques will probably further demonstrate the value of the water channel as a research tool.

RECOMMENDATIONS

(1) All models should be formed from brass for better flow conditions and more accurate construction. Although a mahogany model slides smoothly on the glass bottom, it is impossible to machine its surfaces as smoothly as brass or reproduce its contours as accurately as in the case of a brass model.

(2) It is believed, by visual observation, that the probes are placed too far from the side of the model. Figure 33 depicts the location of a probe as it was placed in these experiments. It can be seen that the probe should define the water depth at point A but at present it appears to measure the depth of the rise in water at a point where the rise has begun to fall off. The purpose of placing the probes 0.1 inch from the side of the model is to avoid the meniscus effect. It is unlikely that the water, particularly in the stale stage, has a meniscus of 0.1 inch. It is therefore recommended that an investigation of the meniscus around the model be made and the probes be replaced accordingly.

(3) A study of the aerodynamic phenomena for an airfoil at a Mach number of unity should be conducted. Although the tests reported in this thesis validate transonic observations, an investigation at a Mach number of one would probably substantiate transonic studies at a point of considerable interest.

(4) Although of little value, a study in the water channel of an airfoil with a detached shock would be extremely interesting if adequate comparison data were available. A method suggested by

Ferri[27] of evaluating pressure drag for flows with detached shocks from the shadow picture taken from above the model could be used.

---

27 Antonio Ferri, "Method for Evaluating from Shadow or Schlieren Photographs the Pressure Drag in Two-dimensional or Axially Symmetrical Flow with Detached Shock". NACA TM No. 1808, 1949.

BIBLIOGRAPHY

A. Fundamental Theory

Courant, Richard, and K. O. Friedrichs, Supersonic Flow and Shock Waves. New York: Interscience Publishers, Inc., 1948. 464 pp.

Ferri, Antonio, Elements of Aerodynamics of Supersonic Flows. New York: The Macmillan Company, 1949. 434 pp.

Hunsaker, Jerome Clarke, and B. G. Rightmire, Engineering Applications of Fluid Mechanics. New York: McGraw-Hill Book Co., 1947. 494 pp.

Lamb, Horace, Hydrodynamics. Sixth Edition: London: Cambridge University Press, 1932. 738 pp.

Liepmann, Hans Wolfgang, and Allen E. Puckett, Introduction to Aerodynamics of a Compressible Fluid. New York: John Wiley and Sons, Inc., 1947. 262 pp.

Rouse, Hunter, Elementary Mechanics of Fluids. New York: John Wiley and Sons, Inc., 1946. 376 pp.

Sibert, Harold Ward, High-Speed Aerodynamics. New York: Prentice-Hall, Inc., 1948. 289 pp.

Streeter, Victor Lyle, Fluid Dynamics. New York: McGraw-Hill Book Co., 1948. 263 pp.

B. The Hydraulic Analogy

Binnie, A. M. and S. G. Hooker, "The Flow Under Gravity of an Incompressible and Inviscid Fluid Through a Constriction in a Horizontal Channel," Proceedings of the Royal Society, 159: 592-608, 1937.

Bruman, J. R. "Application of the Water Channel-Compressible Gas Analogy". North American Aviation, Inc., Engineering Report, No. NA-47-87, 1947. 60 pp.

Catchpole, Eric John, "The Application of the Hydraulic Analogy to Study the Performance of Two Airfoils in Compressible Flow". Unpublished Master's thesis, Georgia Institute of Technology, Atlanta, 1949. 62 pp.

Einstein, H. A. and E. H. Baird, "Progress Report of the Analogy Between Surface Shock Waves on Liquids and Shocks in Compressible Gases". California Institute of Technology Hydrodynamics Laboratory Report. No. N-54, 1946. 68 pp.

Hatch, John Elmer, Jr., "The Application of the Hydraulic Analogies to Problems of Two-Dimensional Compressible Gas Flow". Unpublished Master's thesis, Georgia Institute of Technology, Atlanta, 1949. 57 pp.

Kantrowitz, Arthur, "The Formation and Stability of Normal Shock Waves in Channel Flows". U.S. National Advisory Committee for Aeronautics Technical Note No. 1225, 1947. 41 pp.

Orlin, W. James, Norman J. Linder, and Jack G. Bitterly, "Application of the Analogy Between Water Flow with a Free Surface and TwO-Dimensional Compressible Gas Flow". U.S. National Advisory Committee for Aeronautics Technical Note No. 1185, 1947. 20 pp.

Preiswerk, Ernst, "Application of the Methods of Gas Dynamics to Water Flows with Free Surface".
Part I. "Flows with No Energy Dissipation". U.S. National Advisory Comittee for Aeronautics Technical Memorandum No. 934, 1940. 69 pp.
Part II. "Flows with Momentum Discontinuities (Hydraulic Jumps)". U.S. National Advisory Committee for Aeronautics Technical Memorandum No. 935, 1940. 56 pp.

Riabouchinsky, D., "Mecanique des Fluides - Sur l'analogie hydraulique des movements d'un fluide compressible". Comptes Rendus, 195: 998-9. Paris, 1932.

Thomas, Gerald B., "Application of Water Channel-Compressible Gas Analogies to Problems of Supersonic Wind Tunnel Design". Unpublished Master's thesis, Georgia Institute of Technology, Atlanta, 1949. 55 pp.

C. High Speed Wind Tunnel Test Results

Beavan, J. A., G. A. M. Hyde, and R. G. Fowler, "Pressure and Wake Measurements up to Mach Number 0.85 on an EC1250 Section with 25 per cent. Control". British Aeronautical Research Council Reports and Memoranda No. 2065, 1942. 46 pp.

Ferri, Antonio, "Investigations and Experiments in the Guidonia Supersonic Wind Tunnel". U.S. National Advisory Committee for Aeronautics Technical Memorandum No. 901, 1939. 19 pp.

Ferri, Antonio, "Experimental Results with Airfoils Tested in the High-Speed Tunnel at Guidonia". U.S. National Advisory Committee for Aeronautics Technical Memorandum No. 946, 1940. 14 pp.

Ferri, Antonio, "Completed Tabulation in the United States of Tests of 24 Airfoils at High Mach Numbers". U.S. National Advisory Committee for Aeronautics Wartime Report No. L-143. 21 pp.

Graham, Donald J., Gerald E. Nitzberg, and Robert N. Olson, "A Systematic Investigation of Pressure Distributions at High Speeds over Five Representative NACA Low-Drag and Conventional Airfoil Sections". U.S. National Advisory Committee for Aeronautics Technical Report No. 832, 1945. 68 pp.

Hilton, W. F., "High-Speed Tunnel Balance Tests on N.A.C.A. 2218 Aerofoil". British Aeronautical Research Committee Reports and Memoranda No. 1975, 1943. 4 pp.

_____, "Subsonic and Supersonic Tests on 7½ per cent. Bi-convex Aerofoil". British Aeronautical Research Council Reports and Memoranda No. 2196, 1944. 8 pp.

_____, "An Experimental Analysis of the Forces on Eighteen Aerofoils at High Speeds". British Aeronautical Research Council Reports and Memoranda No. 2058, 1946. 57 pp.

_____, and F. W. Pruden, "Subsonic and Supersonic High Speed Tunnel Tests of a Faired Double Wedge Aerofoil". British Aeronautical Research Council Reports and Memoranda No. 2057, 1943. 13 pp.

Knackstedt, W., "Examination and Evaluation of the Available Results with High-Velocity Flows". Headquarters Air Material Command Wright Field, Dayton, Ohio, Technical Report No. F-TS-1526-RE, 1947. 116 pp.

Liepmann, H. W., H. Askenas, and J. D. Cole, "Experiments in Transonic Flow". United States Air Force Air Material Command Wright-Patterson Air Force Base, Dayton, Ohio, Technical Report No. 5667, 126 pp.

Lindsey, W. F., Bernard N. Daley, and Milton D. Humphreys, "The Flow and Force Characteristics of Supersonic Airfoils at High Subsonic Speeds". U.S. National Advisory Committee for Aeronautics Technical Note No. 1211, 1947. 15 pp.

Pearcey, H. H., "Drag Measurements on N.A.C.A. 2218 Section at Compressibility Speeds for Comparison with Flight Tests and Theory". British Aeronautical Research Council Reports and Memoranda No. 2093, 1943. 9 pp.

Stack, John, and Albert E. von Doenhoff, "Tests of 16 Related Aerofoils at High Speeds". U.S. National Advisory Committee for Aeronautics Technical Report No. 492, 1934. 23 pp.

D. Other References

Bonney, E. Arthur, "Aerodynamic Characteristics of Rectangular Wings at Supersonic Speeds", Journal of the Aeronautical Sciences, 14: 110-16, 1947.

Ferri, Antonio, "Method for Evaluating from Shadow or Schlieren Photographs the Pressure Drag in Two-Dimensional or Axially Symmetrical Flow Phenomena with Detached Shock". U.S. National Advisory Committee for Aeronautics Technical Note No. 1808, 1949. 14 pp.

Page, Leigh, Introduction to Theoretical Physics. New York: D. Van Nostrand Co. Inc., 1928. 482 pp.

APPENDIX I

TABLES

TABLE I

SAMPLE CALCULATION OF PRESSURE COEFFICIENT FROM EXPERIMENTAL DATA

Faired Double Wedge Airfoil, Lower Surface, $\alpha = 0^{\circ}$, $d_s = 0.250$ inch, $d_o = 0.513$ inch

Timer reading = 1.19 seconds, Timer cam length = 2.925 feet

$$\therefore M_s = \frac{\frac{2.925}{1.19}}{\sqrt{g \times \frac{.250}{12}}} = 1.45, \quad \frac{1}{M_s^2} = 0.475$$

$$C_p(\gamma=2.0) = \frac{1}{M_s^2}\left[\left(\frac{d_1}{d_s}\right)^2 - 1\right] \qquad \text{Eqn. (11)}$$

$$C_p(\gamma=1.4) = \frac{1}{M_s^2}\left\{\left[\left(p_1/p_o\right)_{\gamma=1.4} \div \left(p_1/p_o\right)_{\gamma=2.0}\right]^{28}\left(d_1/d_s\right)^2 - 1\right\}$$

(1) Station (% chord)	(2) d_1/d_s	(3) d_1/d_o	(4) $(p_1/p_o)_{\gamma=1.4}$	(5) $(p_1/p_o)_{\gamma=2.0}$	(6) (4)/(5)	(7) $(d_1/d_s)^2$	(8) (6)x(7)	(9) $C_p(\gamma=1.4)$	(10) $C_p(\gamma=2)$
10	1.338	.651	.51	.43	1.19	1.79	2.13	.537	.376
20	1.252	.610	.46	.38	1.21	1.57	1.90	.429	.271
30	1.225	.596	.42	.35	1.20	1.50	1.80	.381	.238
40	1.100	.536	.36	.29	1.24	1.21	1.50	.238	.100
50	0.996	.485	.29	.23	1.26	0.993	1.25	.119	-.003
60	1.024	.499	.31	.25	1.24	1.05	1.30	.143	.024
70	1.020	.497	.31	.25	1.24	1.04	1.29	.138	.019
80	1.024	.499	.31	.25	1.24	1.05	1.30	.143	.024
90	1.096	.534	.36	.29	1.24	1.20	1.49	.233	.095

[28] James Orlin, Norman J. Linder, and Jack G. Bitterly. op. cit., Fig. 1.

TABLE II

EXPERIMENTAL VALUES OF LIFT, DRAG, AND MOMENT COEFFICIENTS FOR FAIRED DOUBLE WEDGE AIRFOIL

$M = 0.80, \gamma = 2.0$

α (degrees)	C_L	C_D	$C_{M_{\frac{1}{4}}}$
-2	-.162	.040	.002
0	.048	.029	-.024
4	.484	.057	-.032
7	.784	.134	-.016

$M = 0.80, \gamma = 1.4$

α (degrees)	C_L	C_D	$C_{M_{\frac{1}{4}}}$
-2	-.149	.033	.002
0	.042	.025	-.024
4	.442	.052	-.029
7	.736	.115	-.014

$M = 1.21, \gamma = 2.0$

α (degrees)	C_L	C_D	$C_{M_{\frac{1}{4}}}$
-5	-.444	.087	.041
-4	-.406	.079	.036
-2	-.221	.050	.028
0	.029	.046	.006
2	.198	.051	-.025
4	.408	.077	-.036
5	.555	.084	-.049

TABLE II (Cont.)

$M = 1.21, \gamma = 1.4$

α (degrees)	C_L	C_D	$C_{M_{\frac{1}{4}}}$
-5	-.489	.095	.054
-4	-.428	.087	.043
-2	-.235	.055	.028
0	.029	.046	.007
2	.212	.054	-.029
4	.429	.084	-.040
5	.578	.092	-.053

$M = 1.45, \gamma = 2.0$

α (degrees)	C_L	C_D	$C_{M_{\frac{1}{4}}}$
-5	-.306	.063	.056
-4	-.234	.049	.043
-2	-.101	.040	.024
0	-.008	.031	.006
2	.121	.044	-.018
4	.241	.050	-.039

$M = 1.45, \gamma = 1.4$

α (degrees)	C_L	C_D	$C_{M_{\frac{1}{4}}}$
-5	-.321	.066	.054
-4	-.249	.054	.038
-2	-.114	.044	.021
0	.010	.032	.006
2	.134	.049	-.016
4	.253	.057	-.038

TABLE III

EXPERIMENTAL VALUES OF LIFT, DRAG, AND MOMENT

COEFFICIENTS FOR BI-CONVEX AIRFOIL

$M = 0.80, \gamma = 2.0$

α (degrees)	C_L	C_D	$C_{M_{\frac{1}{4}}}$
-4	-.60	.024	-.001
-2	-.30	.014	-.020
0	.00	.008	.000
2	.30	.014	.020
4	.60	.024	.001

$M = 0.80, \gamma = 1.4$

α (degrees)	C_L	C_D	$C_{M_{\frac{1}{4}}}$
-4	-.55	.024	-.001
-2	-.27	.014	-.020
0	.00	.008	.000
2	.27	.014	.020
4	.55	.024	.001

$M = 1.25, \gamma = 2.0$

α (degrees)	C_L	C_D	$C_{M_{\frac{1}{4}}}$
-4	-.452	.057	.056
-2	-.212	.035	.030
0	.000	.033	.000
2	.212	.035	-.030
4	.452	.057	-.056

TABLE III (Cont.)

$M = 1.25, \gamma = 1.4$

α (degrees)	C_L	C_D	$C_{M_{\frac{1}{4}}}$
-4	-.456	.062	-.054
-2	-.215	.039	-.030
0	.000	.037	.000
2	.215	.039	.030
4	.456	.062	.054

TABLE IV

EXPERIMENTAL VALUES OF LIFT, DRAG, AND MOMENT COEFFICIENTS FOR G. U. 4 AIRFOIL

$M = 2.13, \gamma = 2.0$

α (degrees)	C_L	C_D	C_M
-2	-.072	.012	.022
0	.006	.009	.006
2	.040	.011	-.020
6	.181	.022	-.052

$M = 2.13, \gamma = 1.4$

α (degrees)	C_L	C_D	C_M
-2	-.080	.016	.026
0	.007	.013	.007
2	.051	.014	-.025
6	.216	.028	-.060

APPENDIX II

FIGURES

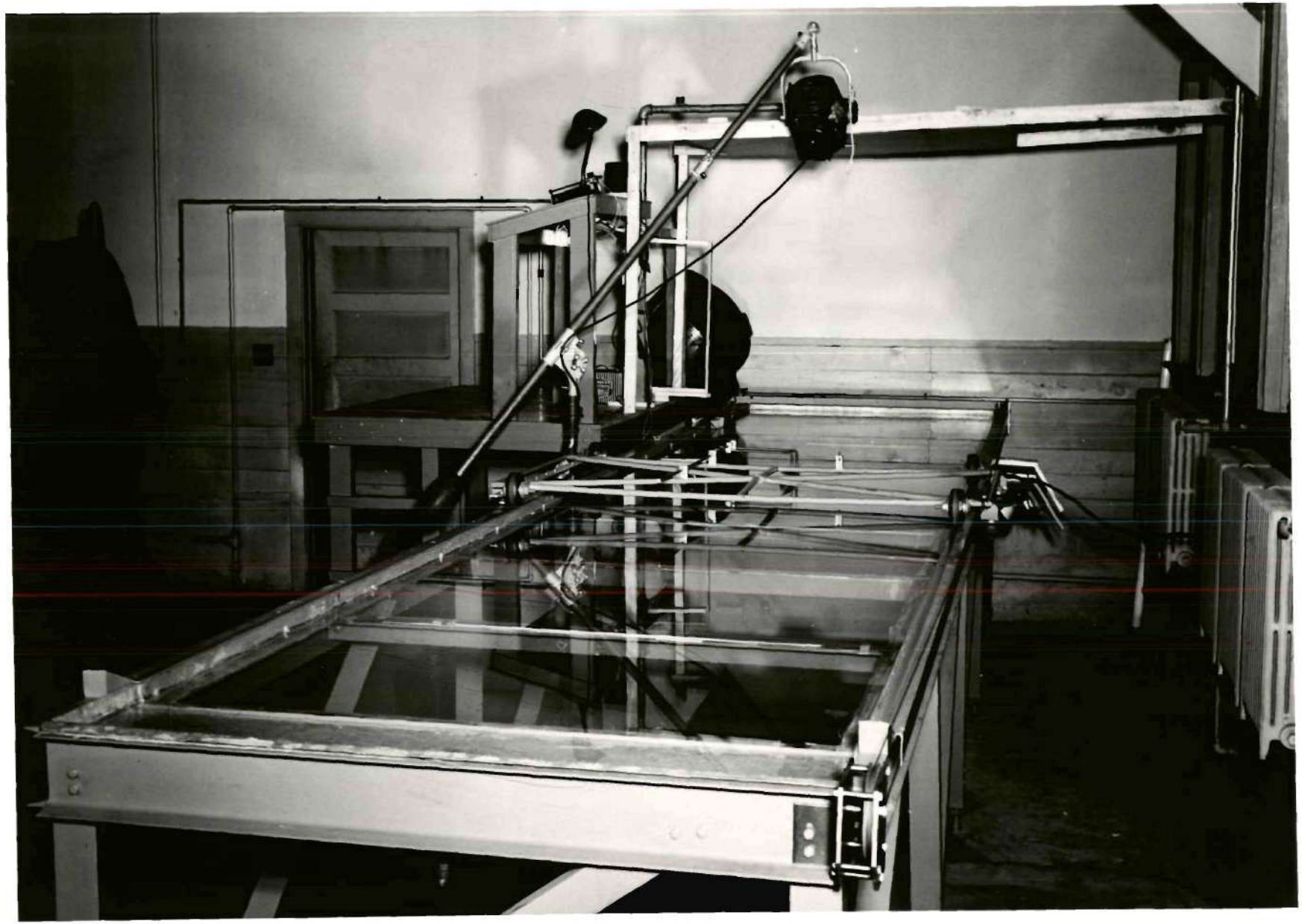

FIGURE 1

GENERAL VIEW OF WATER CHANNEL

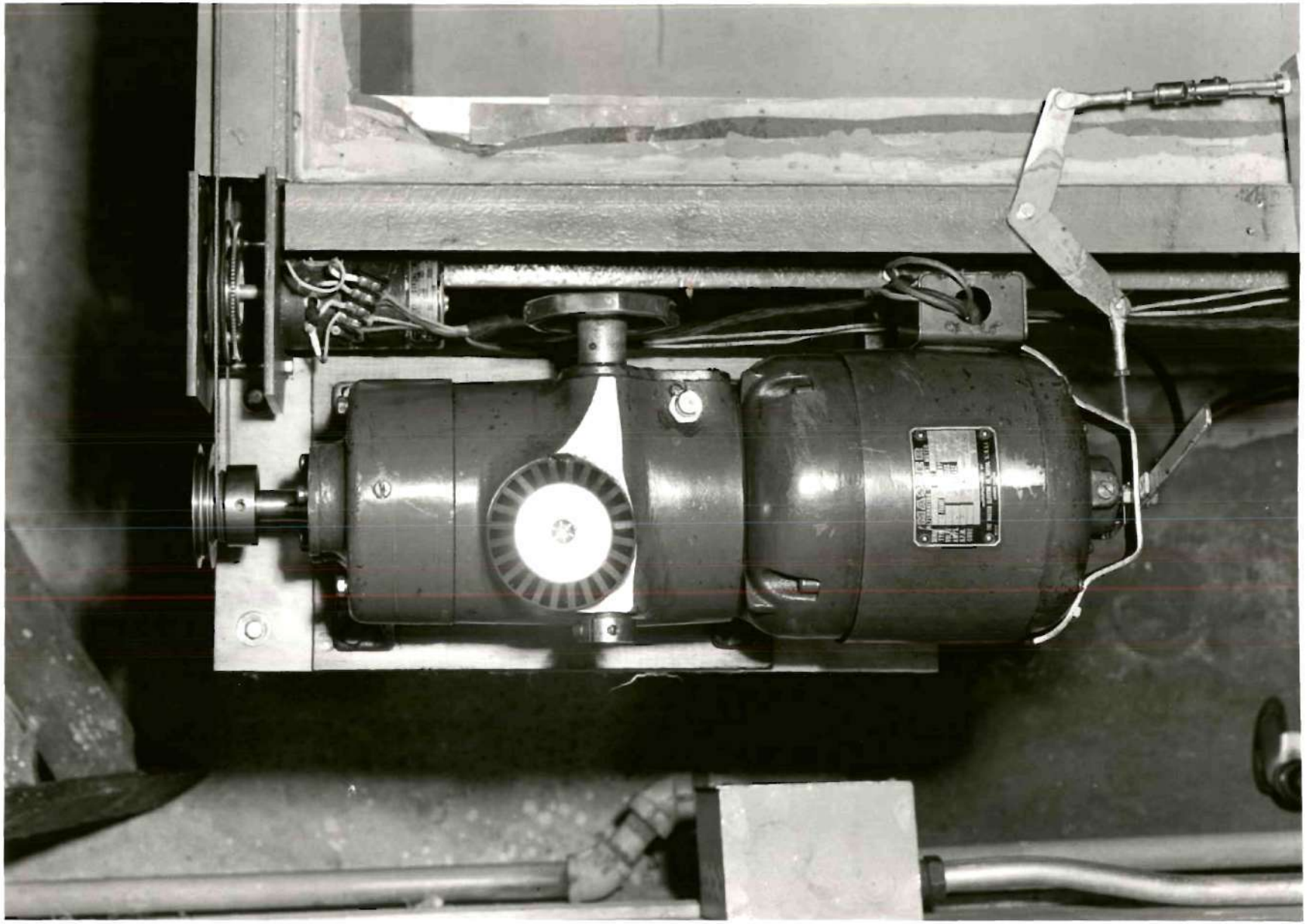

FIGURE 2

CARRIAGE DRIVE MECHANISM

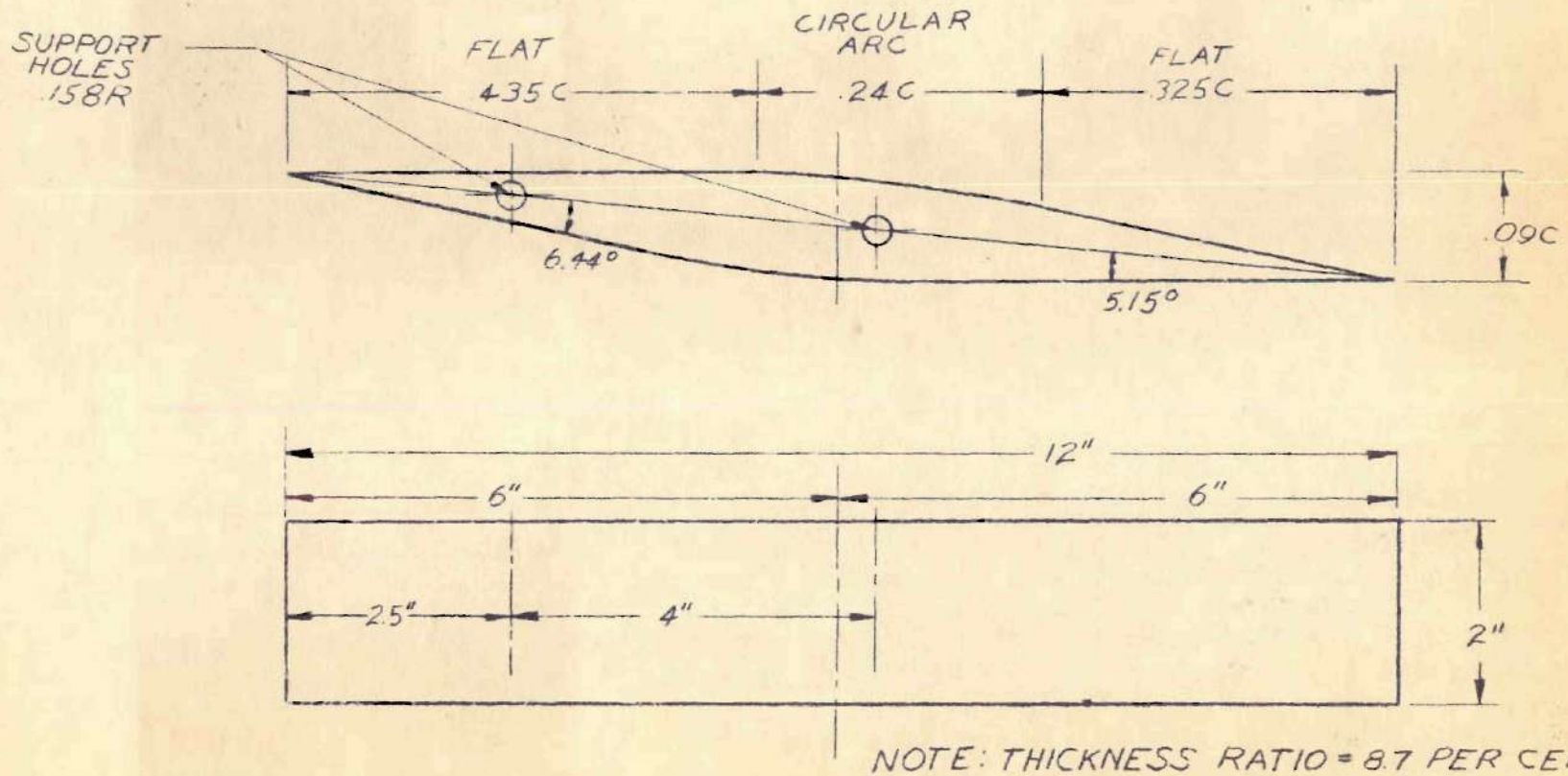

NOTE: THICKNESS RATIO = 8.7 PER CENT.
AIRFOIL HAS FORE AND AFT SYMMETRY.
FLATS ARE TANGENTIAL TO CIRCULAR ARCS.
AIRFOIL SHOWN AT +5.15° INCIDENCE.

FIGURE 3. FAIRED DOUBLE WEDGE AIRFOIL

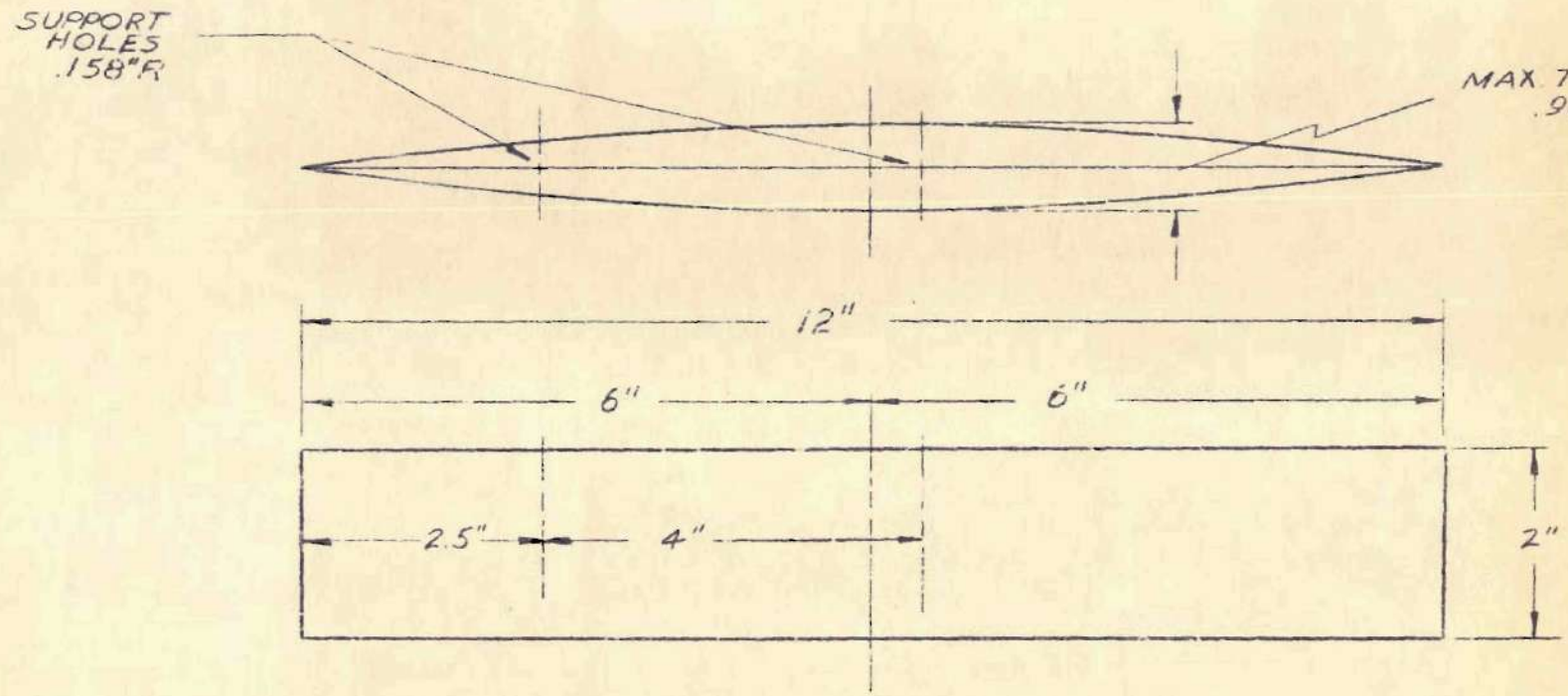

FIGURE 4. BI-CONVEX AIRFOIL

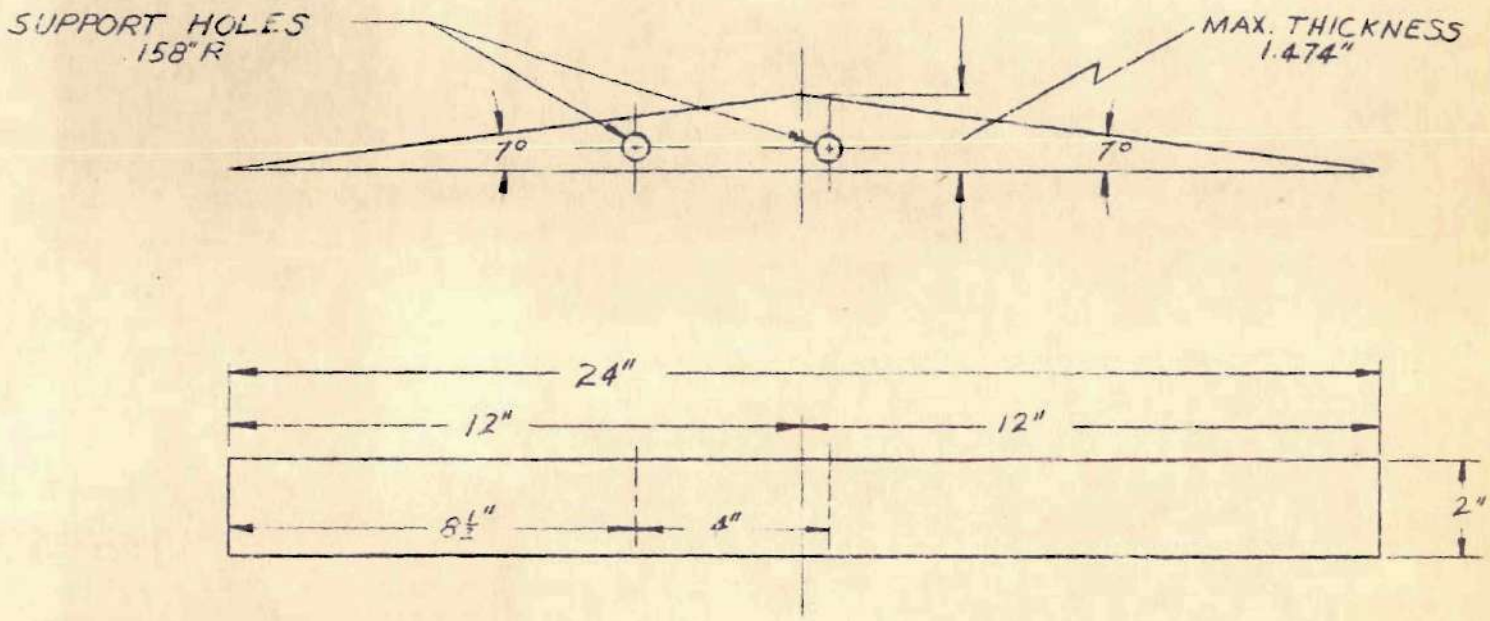

FIGURE 5. G.U. 4 AIRFOIL MODEL

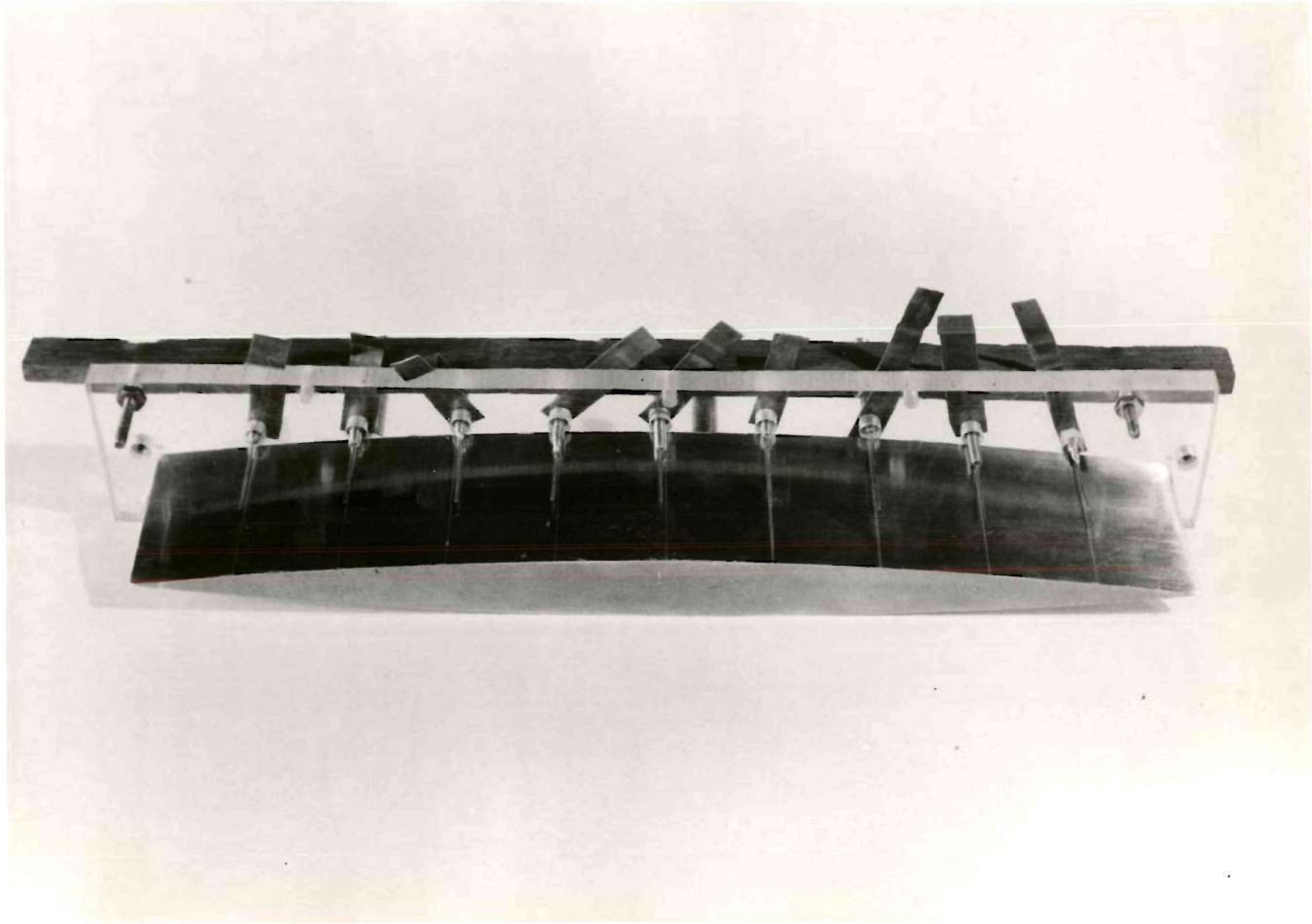

FIGURE 6

VIEW OF MODEL WITH PROBES IN POSITION

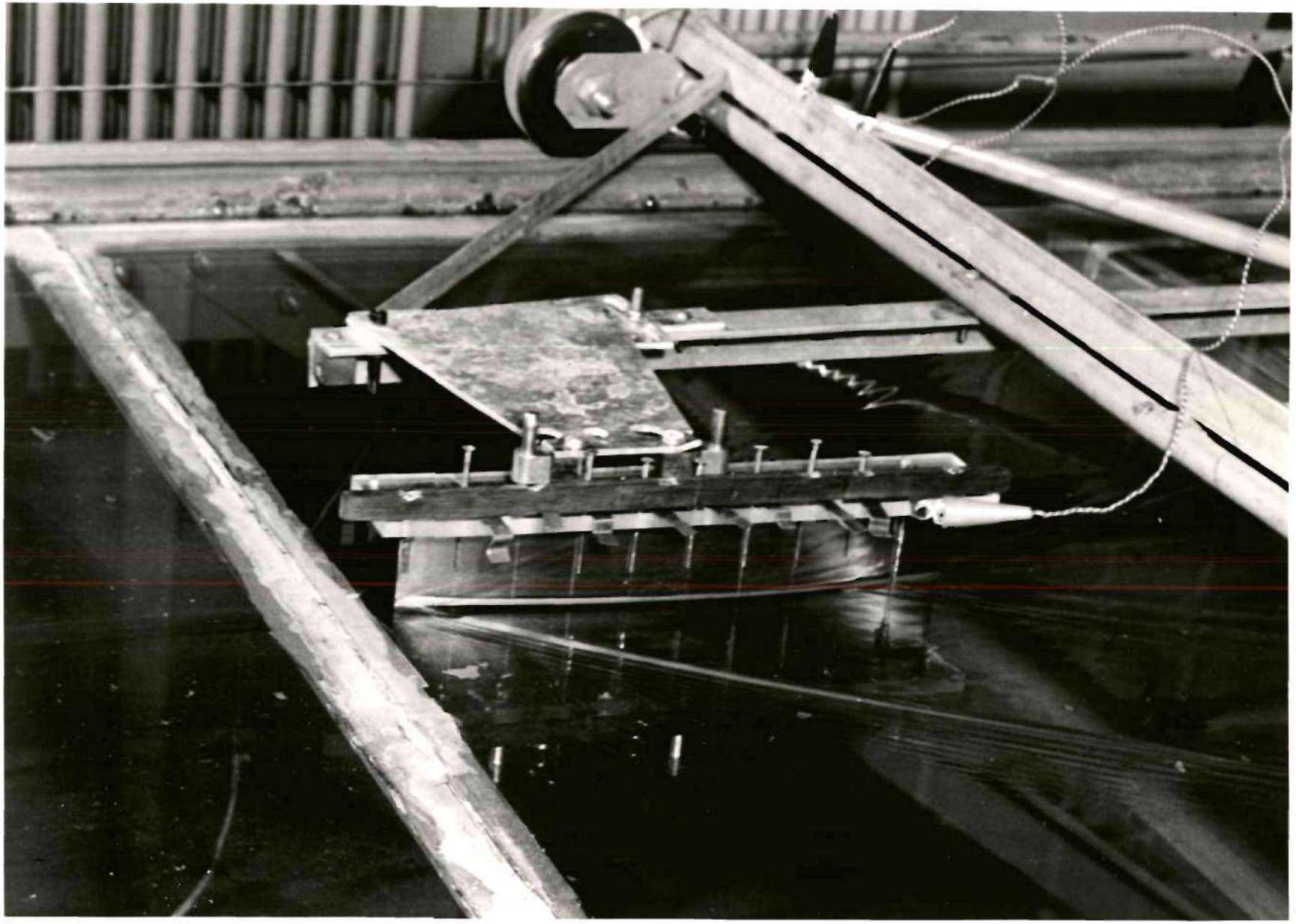

FIGURE 7

FLOW ABOUT BI-CONVEX MODEL

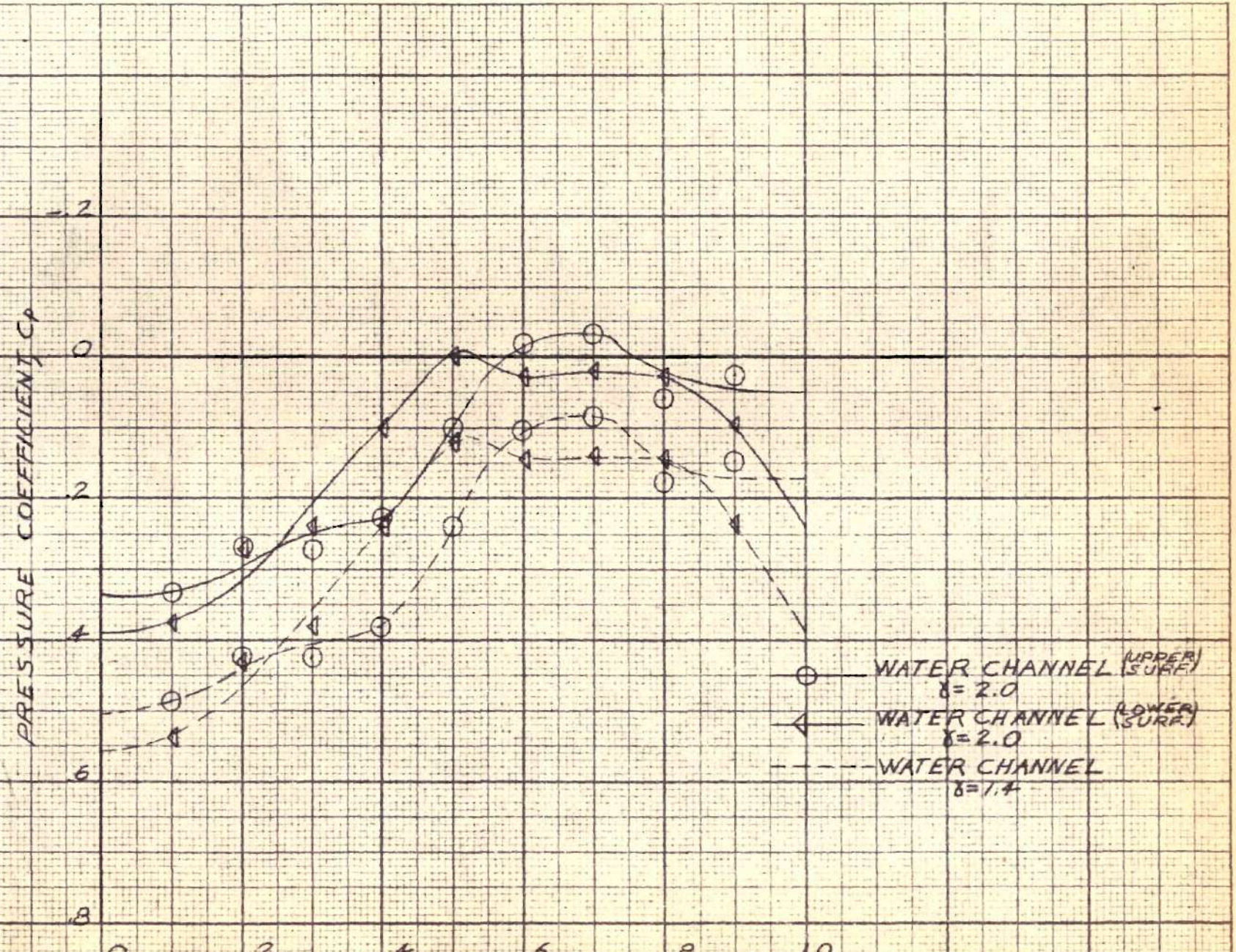

FIGURE 8. - CHORDWISE PRESSURE DISTRIBUTION FOR FAIRED DOUBLE WEDGE AIRFOIL AT $M = 1.45$, $\alpha = 0°$

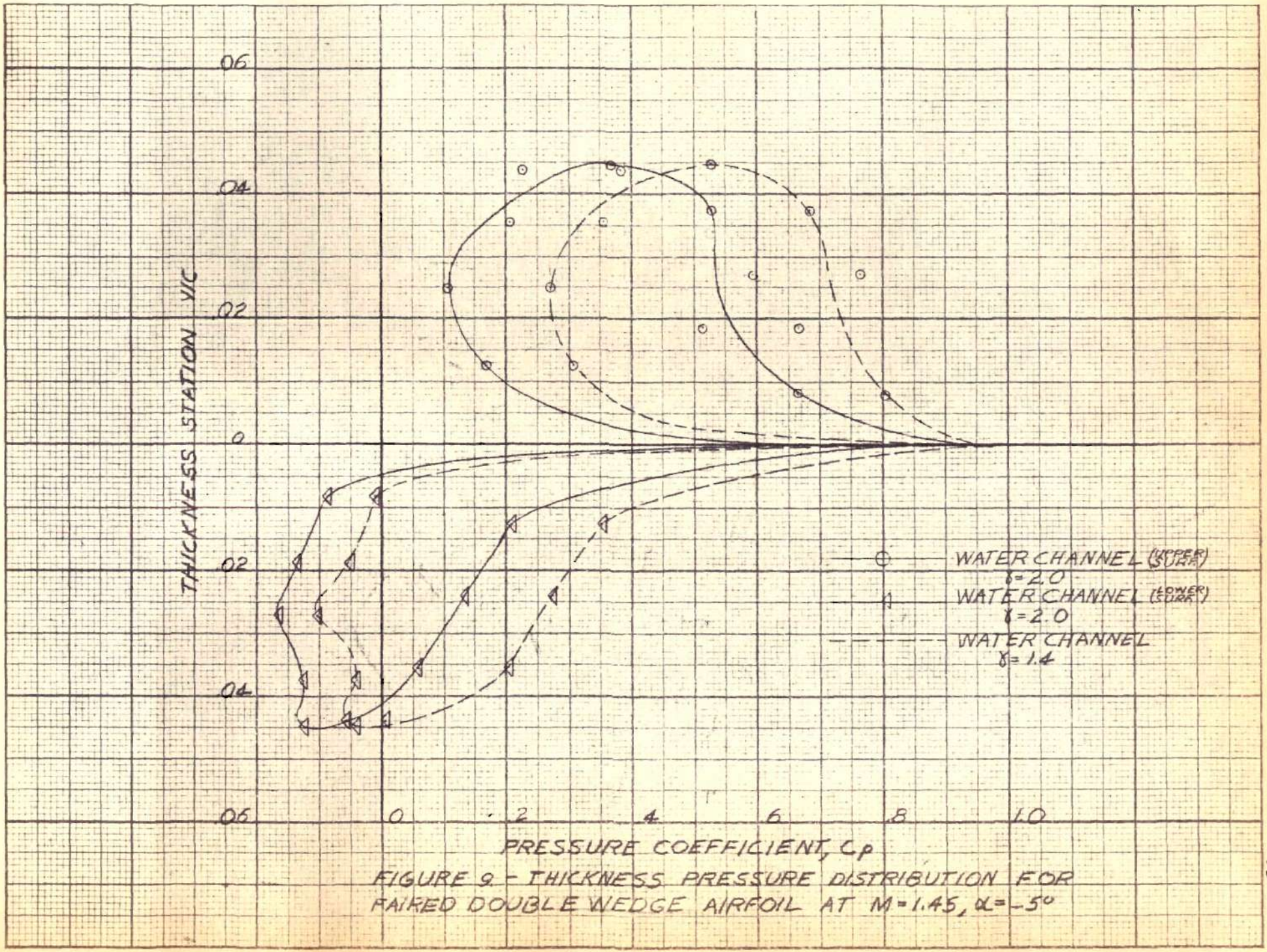

FIGURE 9 - THICKNESS PRESSURE DISTRIBUTION FOR FAIRED DOUBLE WEDGE AIRFOIL AT $M = 1.45$, $\alpha = -5°$

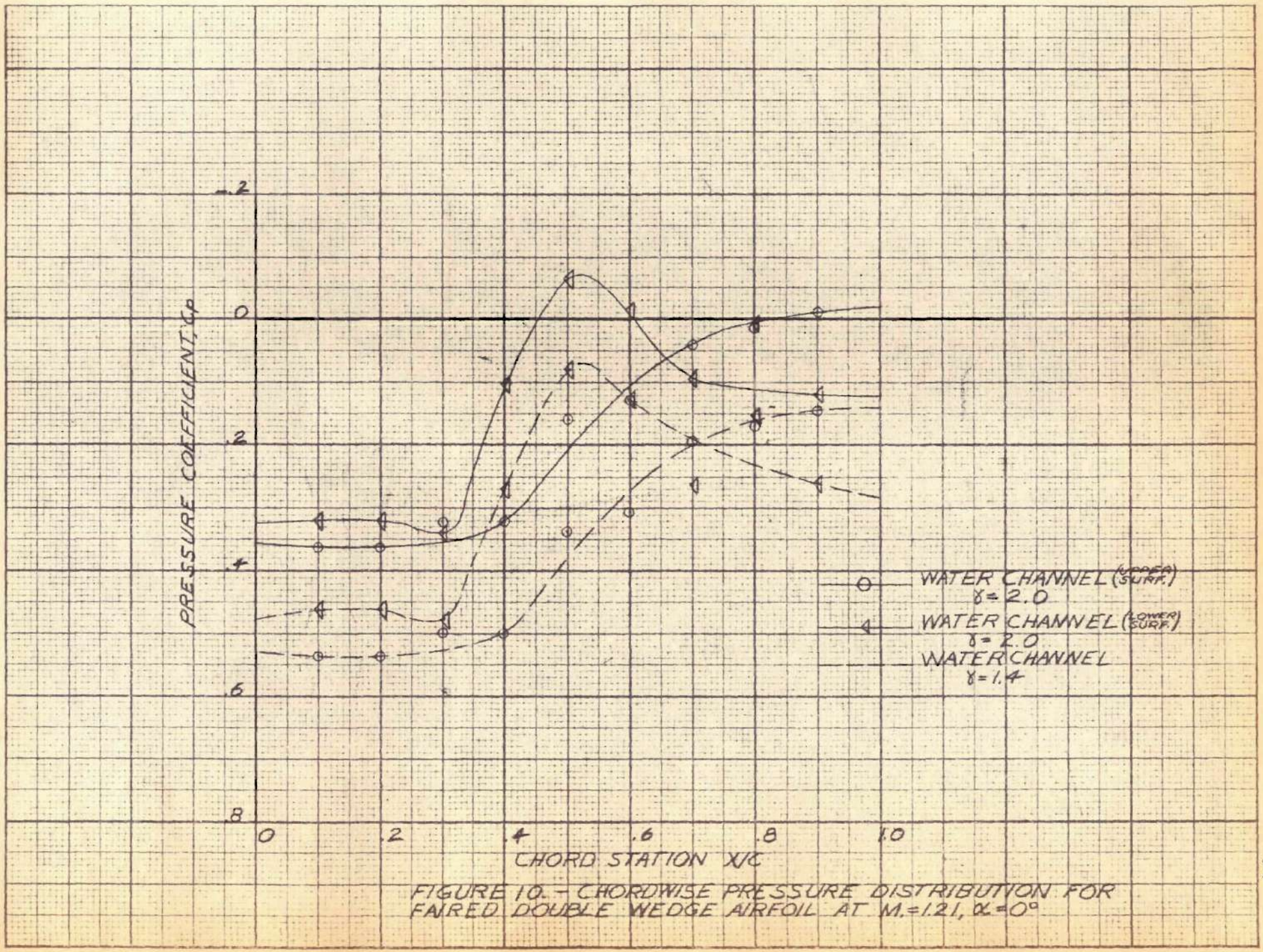

FIGURE 10. - CHORDWISE PRESSURE DISTRIBUTION FOR FAIRED DOUBLE WEDGE AIRFOIL AT M. = 1.21, α = 0°

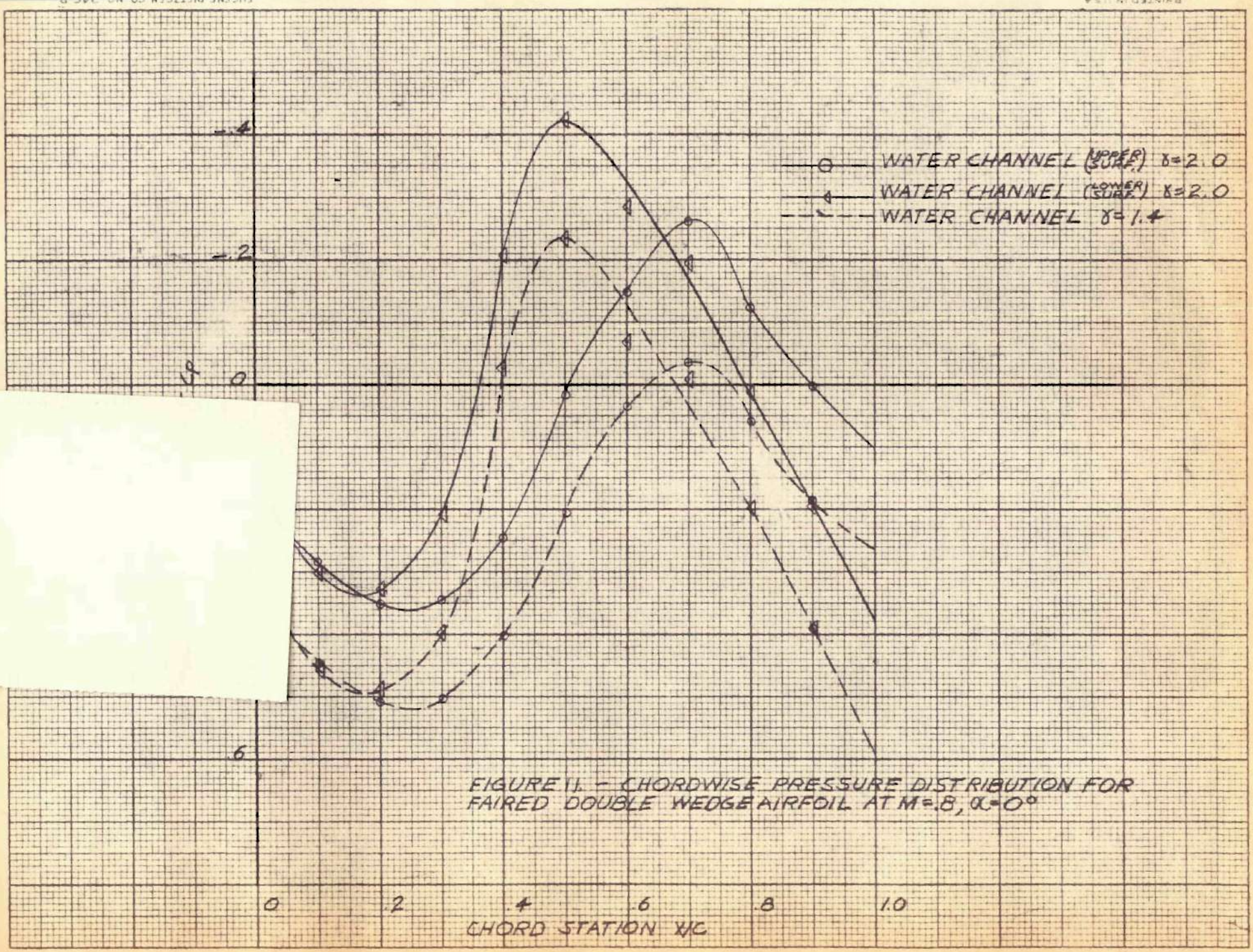

FIGURE 11. – CHORDWISE PRESSURE DISTRIBUTION FOR FAIRED DOUBLE WEDGE AIRFOIL AT M=.8, α=0°

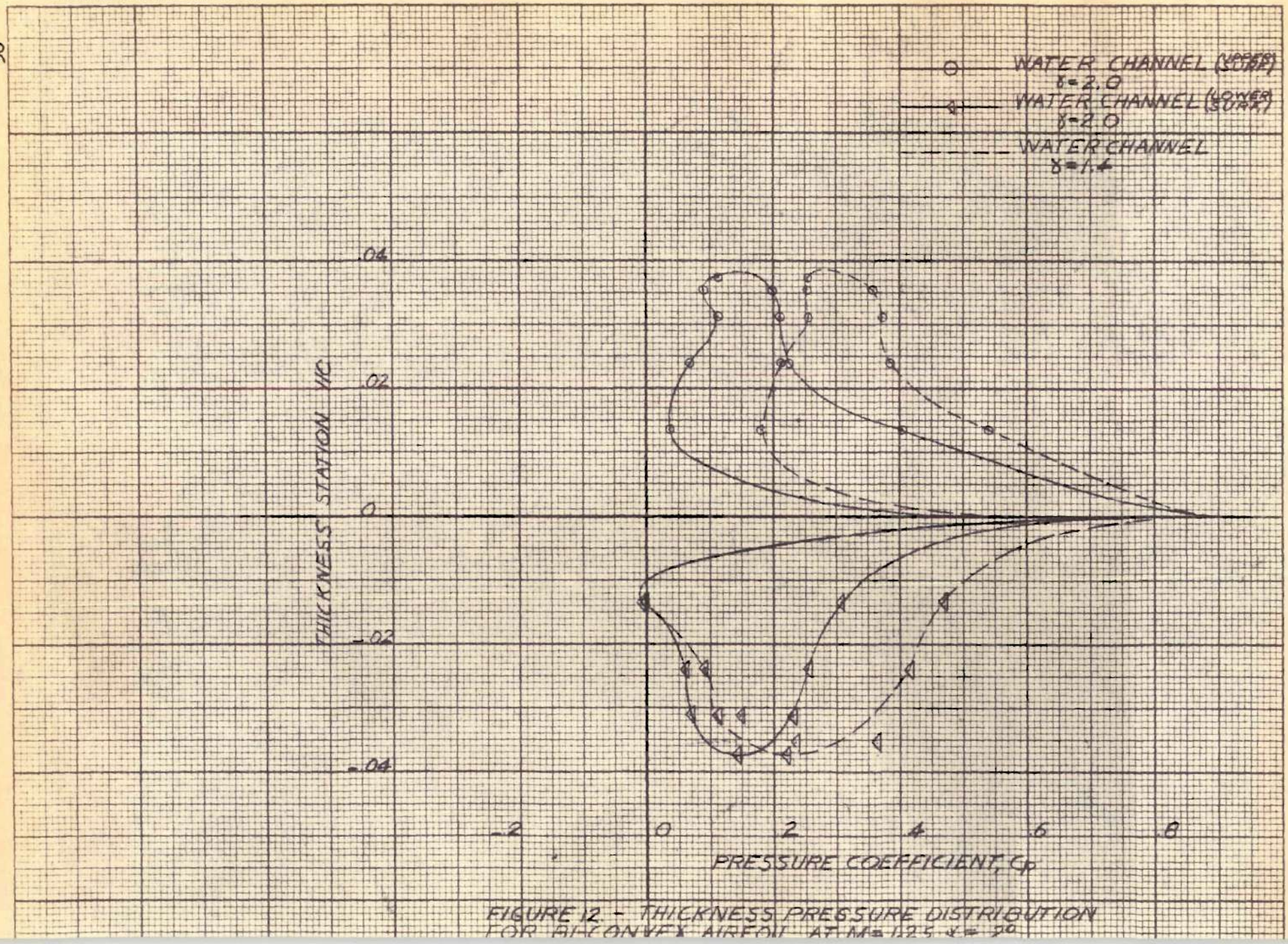

FIGURE 12 - THICKNESS PRESSURE DISTRIBUTION FOR BICONVEX AIRFOIL AT M=.125 α=2°

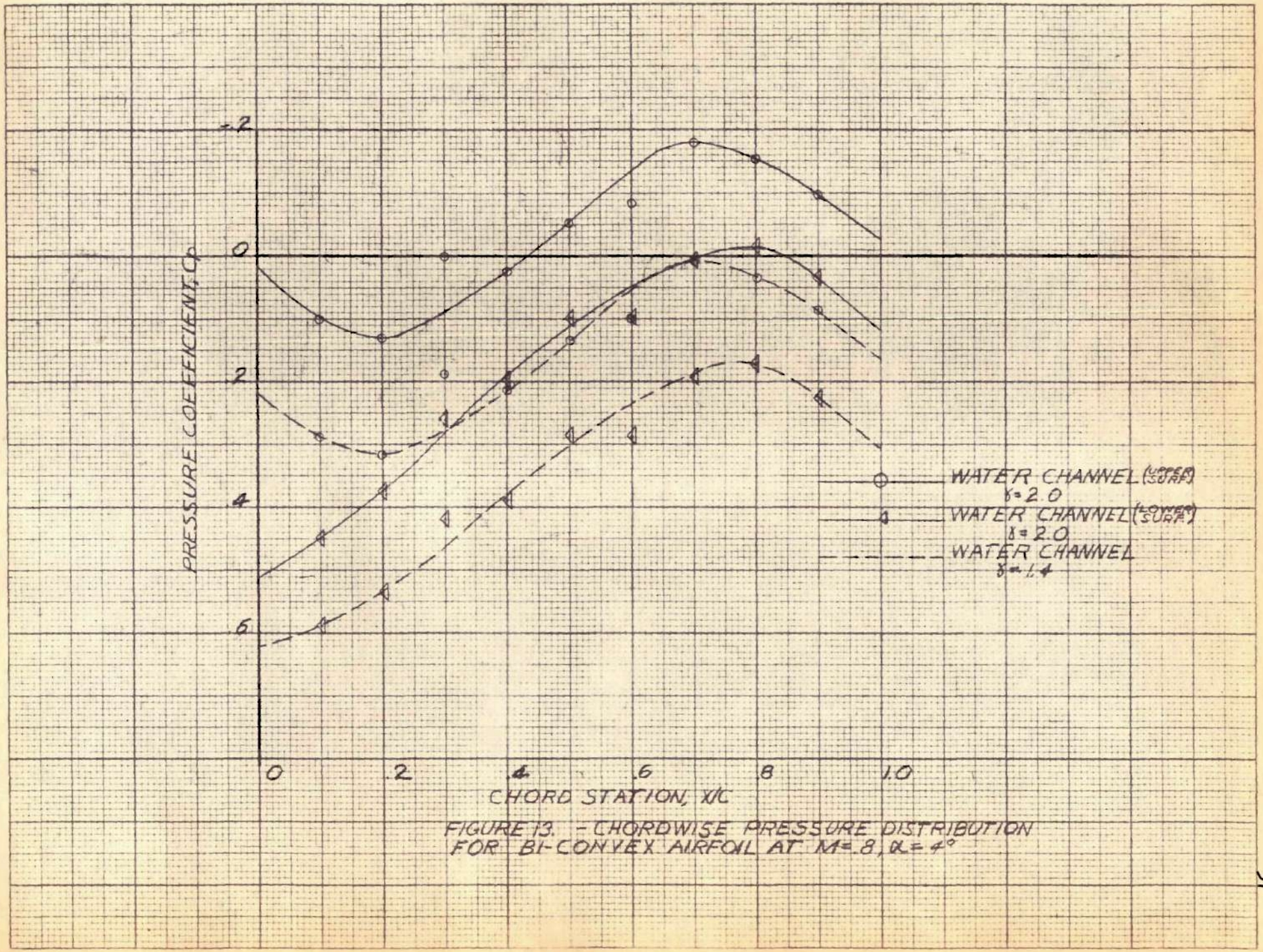

FIGURE 13. - CHORDWISE PRESSURE DISTRIBUTION FOR BI-CONVEX AIRFOIL AT M=.8, α=4°

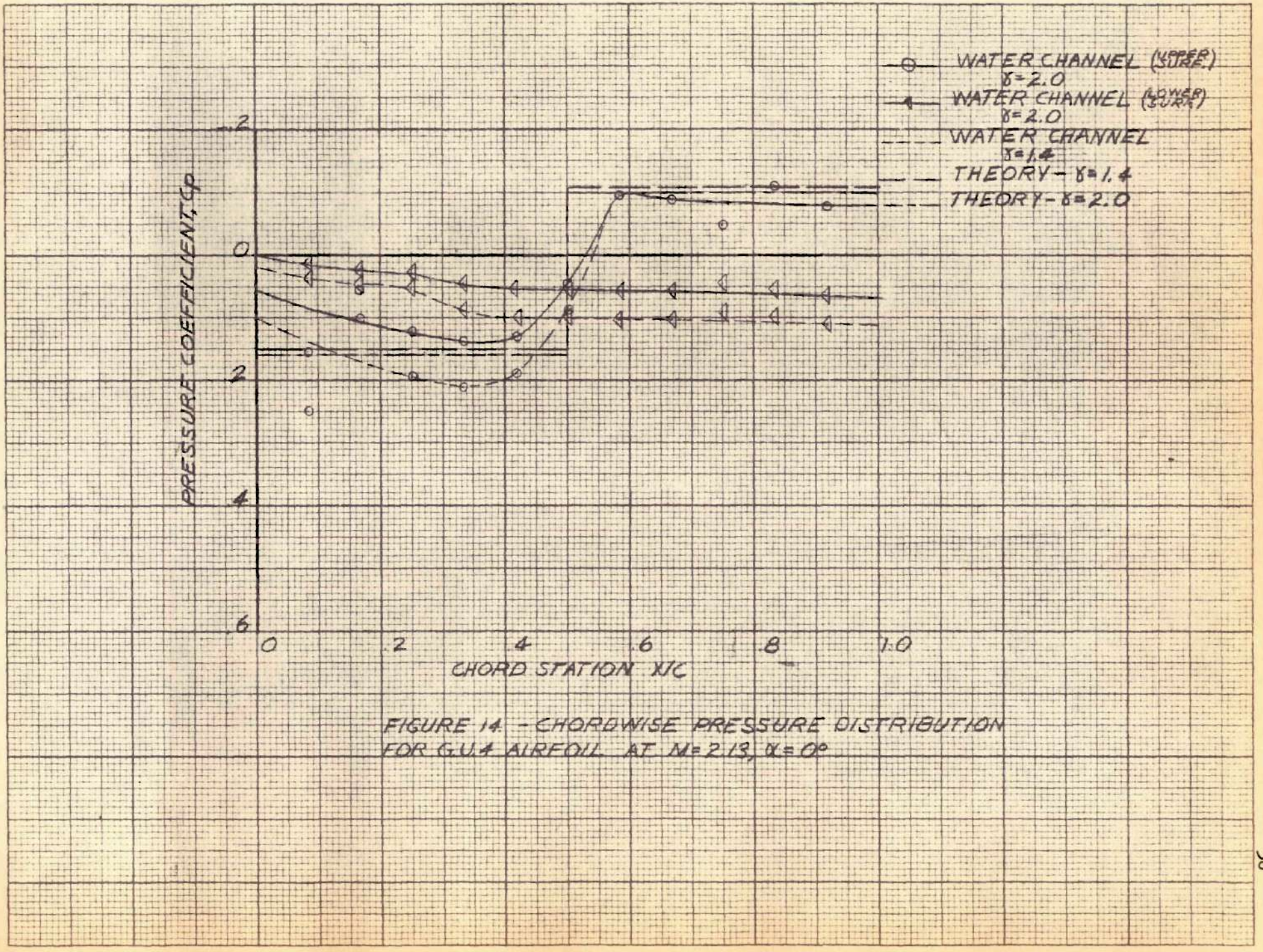

FIGURE 14. - CHORDWISE PRESSURE DISTRIBUTION FOR G.U.4 AIRFOIL AT M=2.13, α=0°

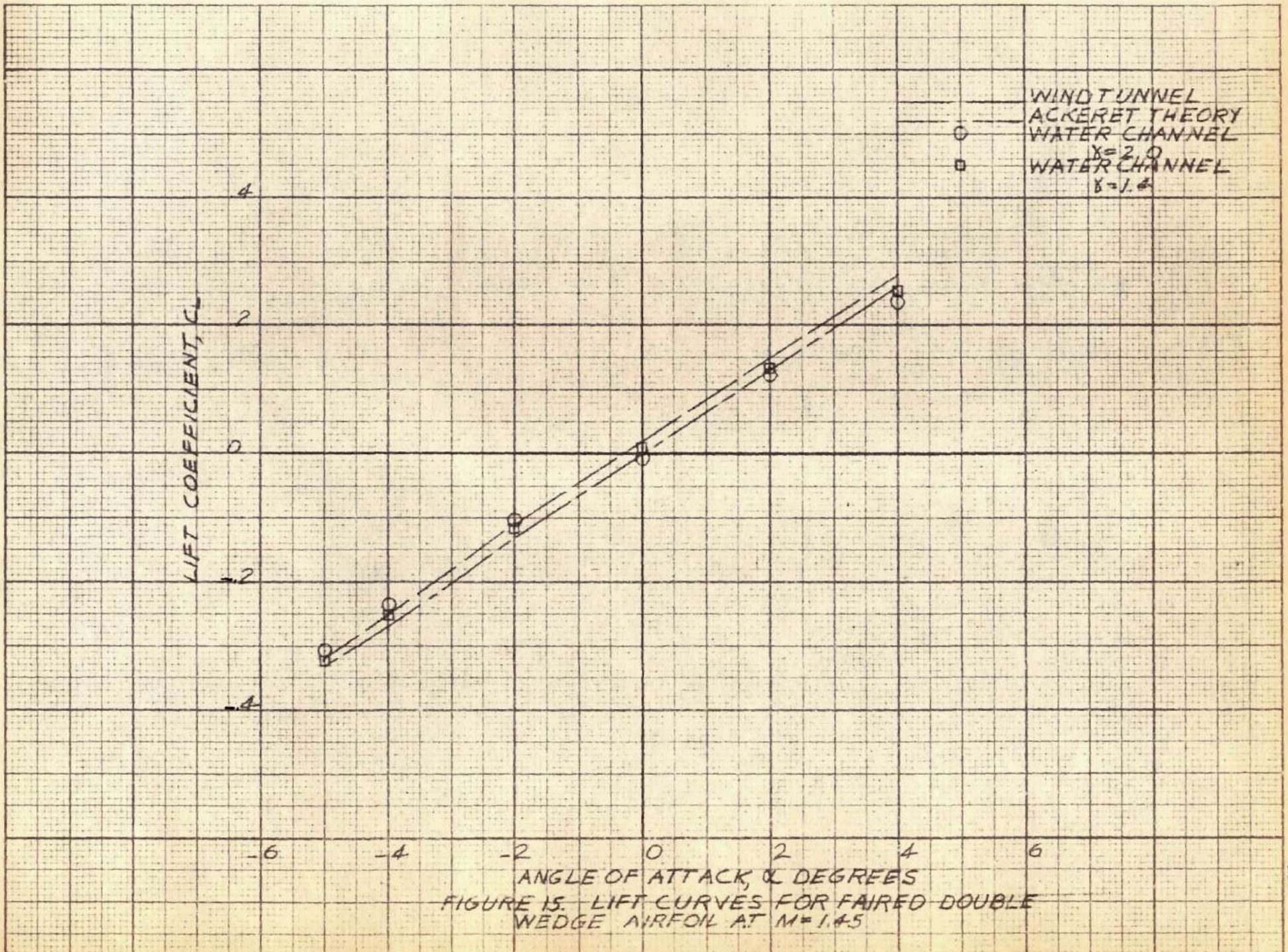

FIGURE 15. LIFT CURVES FOR FAIRED DOUBLE WEDGE AIRFOIL AT M=1.45

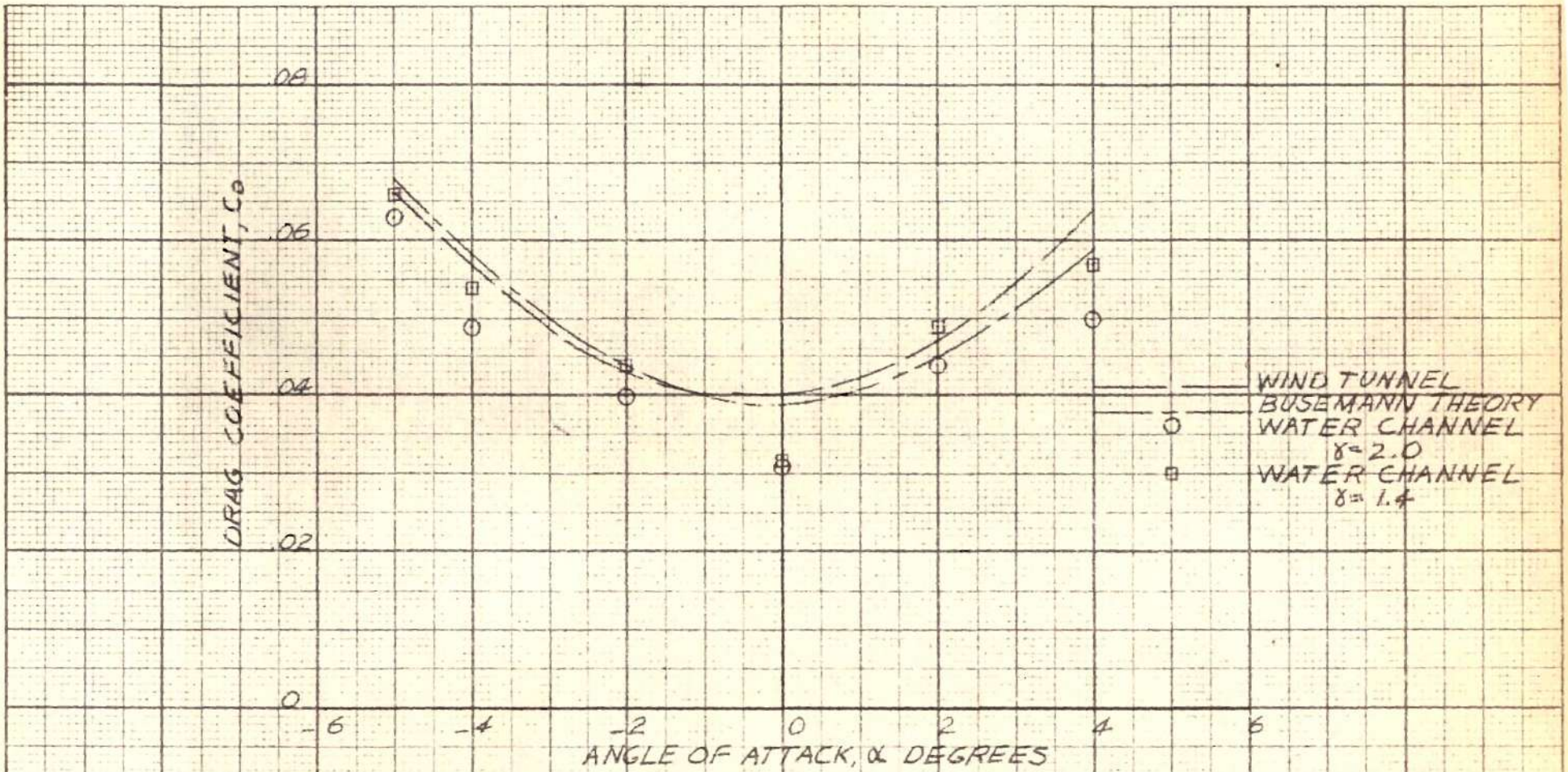

FIGURE 16. DRAG CURVES FOR FAIRED DOUBLE WEDGE AIRFOIL AT $M = 1.45$

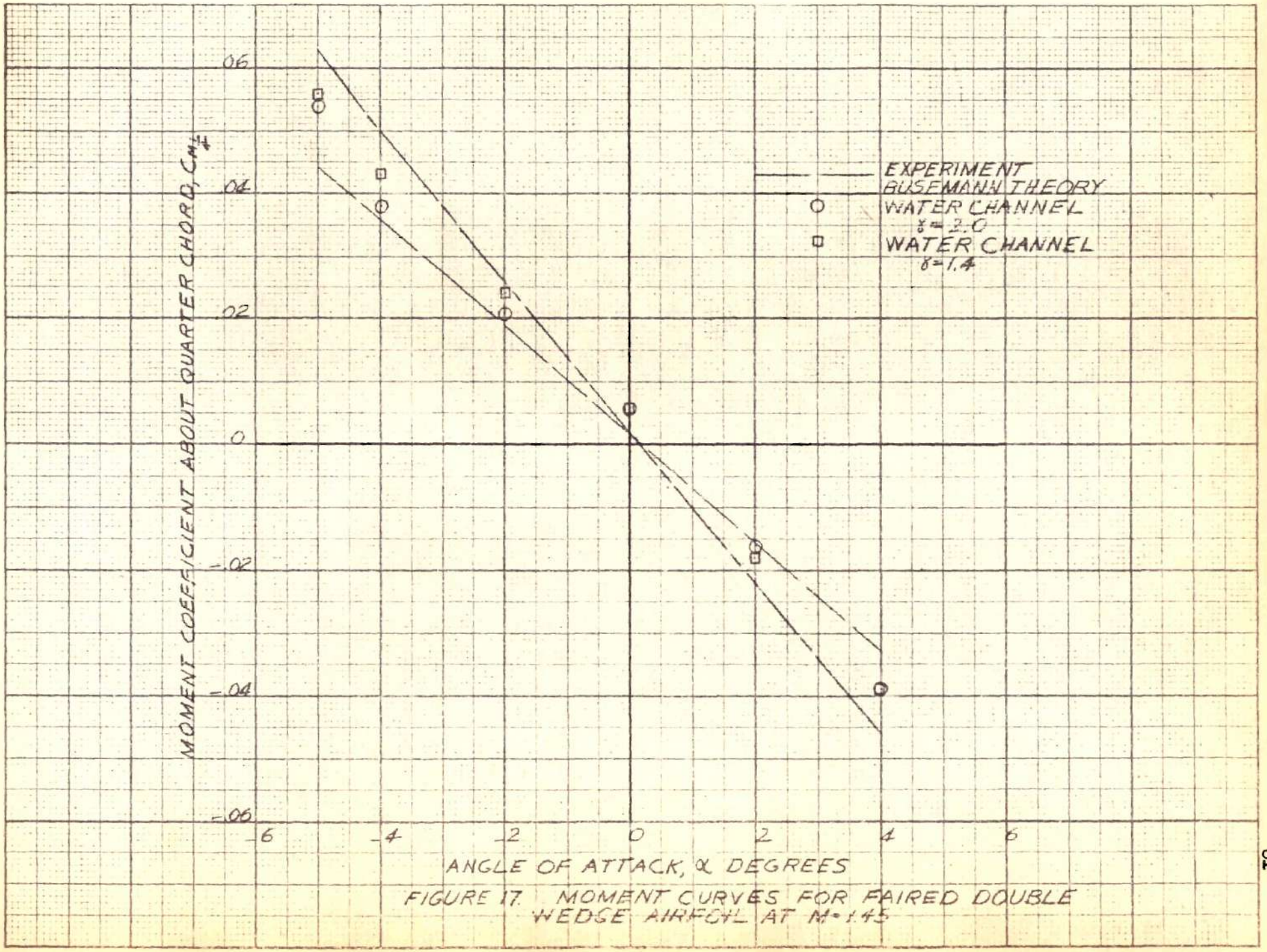

FIGURE 17. MOMENT CURVES FOR FAIRED DOUBLE WEDGE AIRFOIL AT M=1.45

FIGURE 18. LIFT CURVES FOR FAIRED DOUBLE WEDGE AIRFOIL AT M=1.21

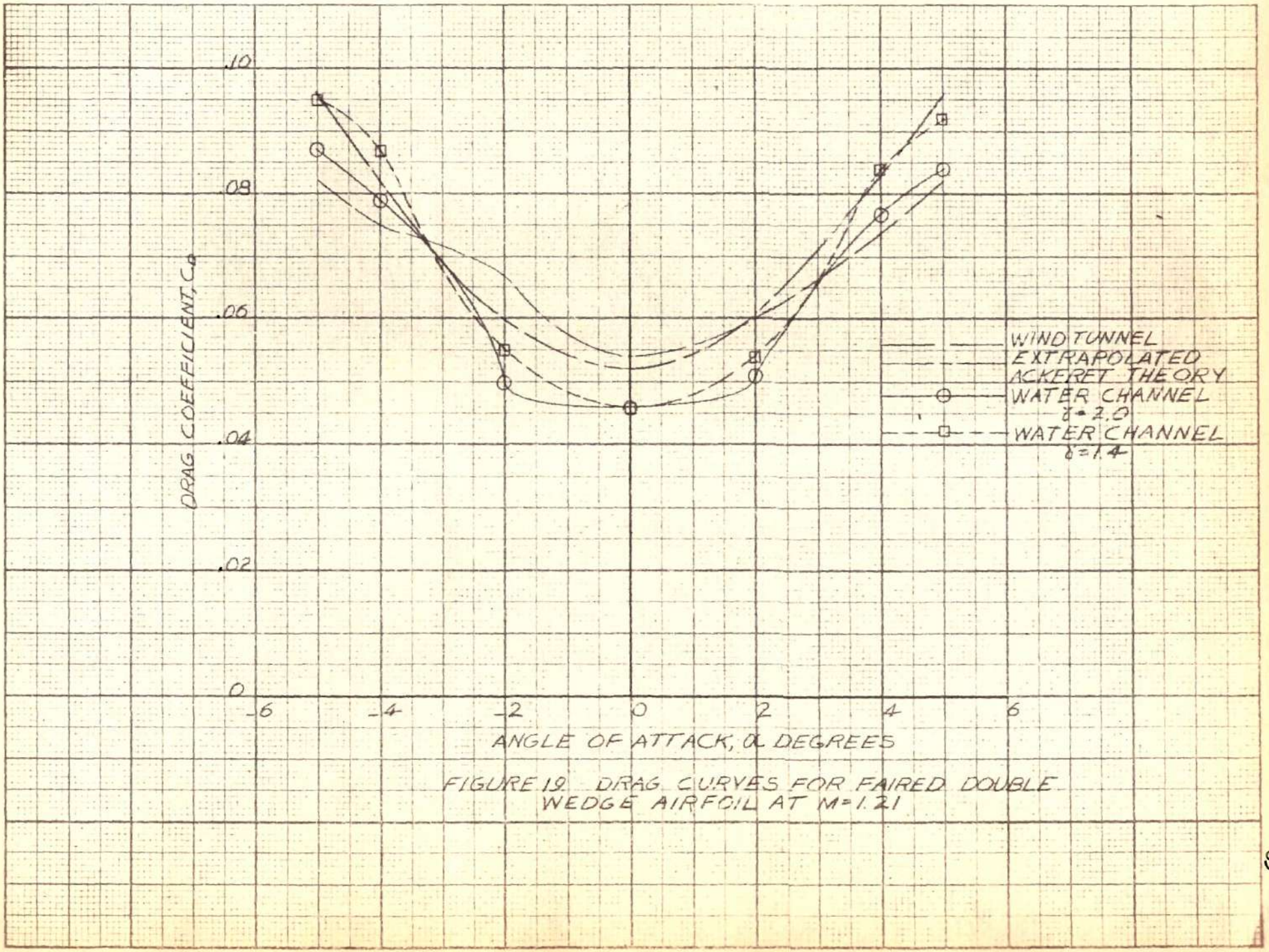

FIGURE 19. DRAG CURVES FOR FAIRED DOUBLE WEDGE AIRFOIL AT M = 1.21

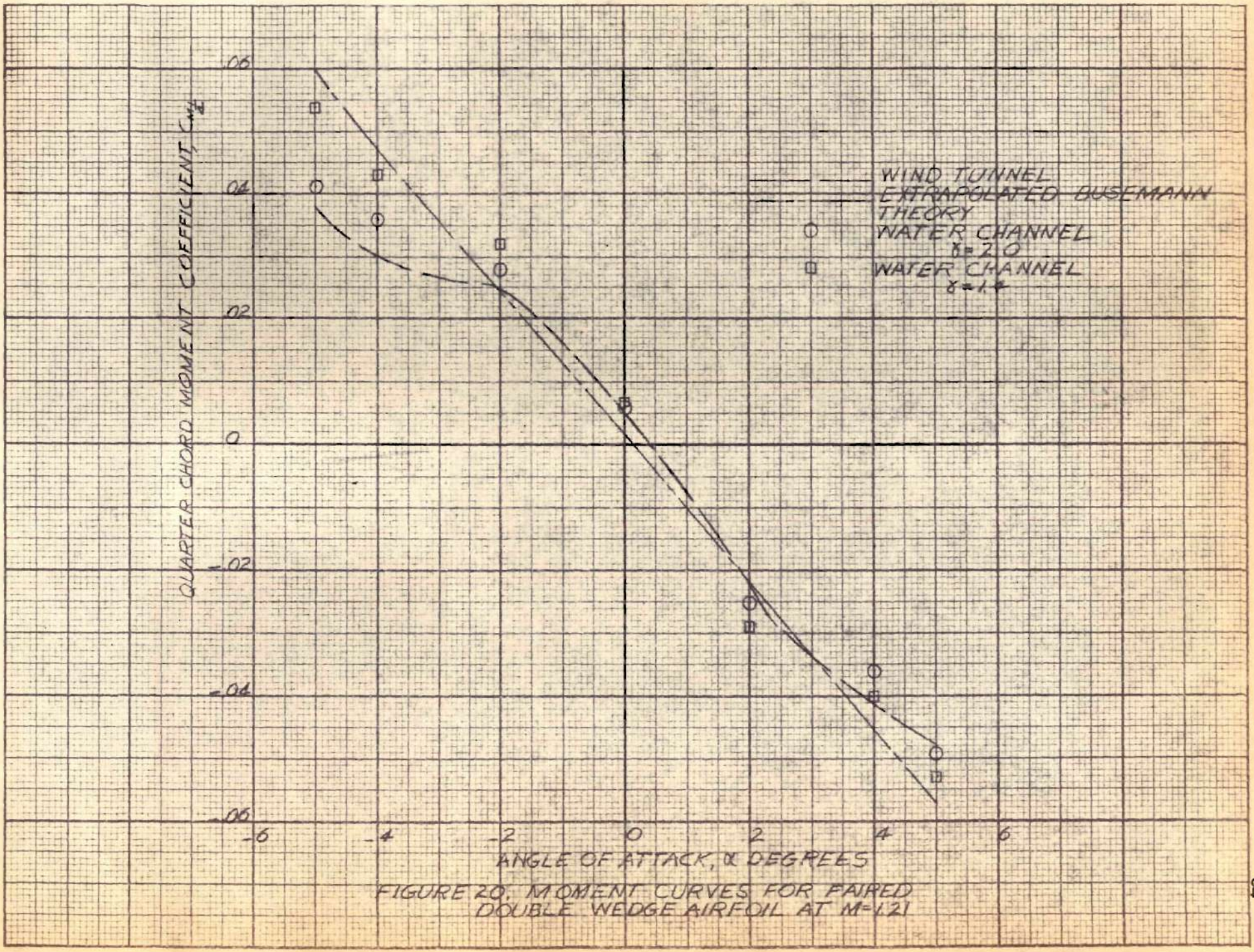

FIGURE 20. MOMENT CURVES FOR FAIRED DOUBLE WEDGE AIRFOIL AT M=1.21

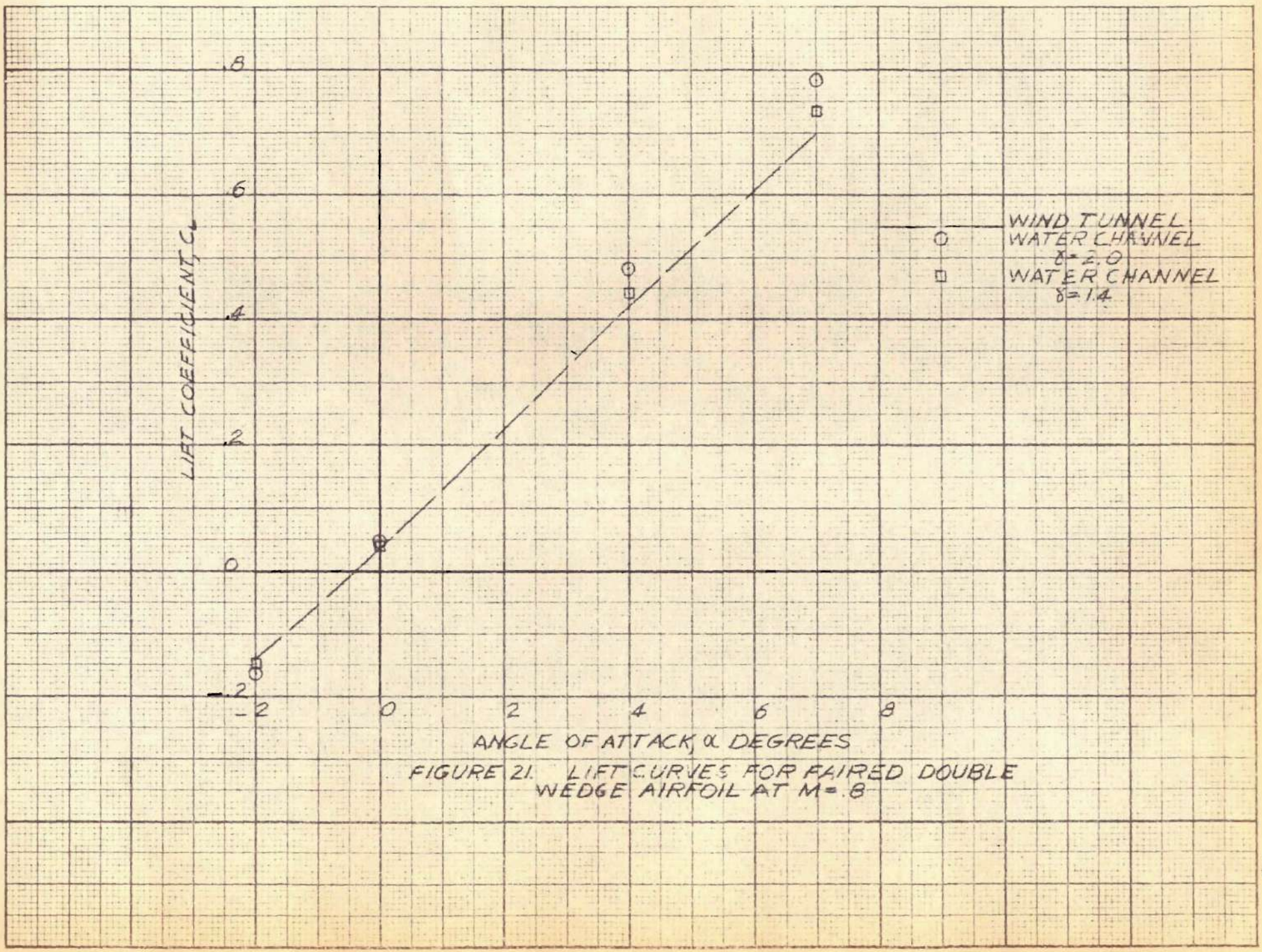

FIGURE 21. LIFT CURVES FOR FAIRED DOUBLE WEDGE AIRFOIL AT M=.8

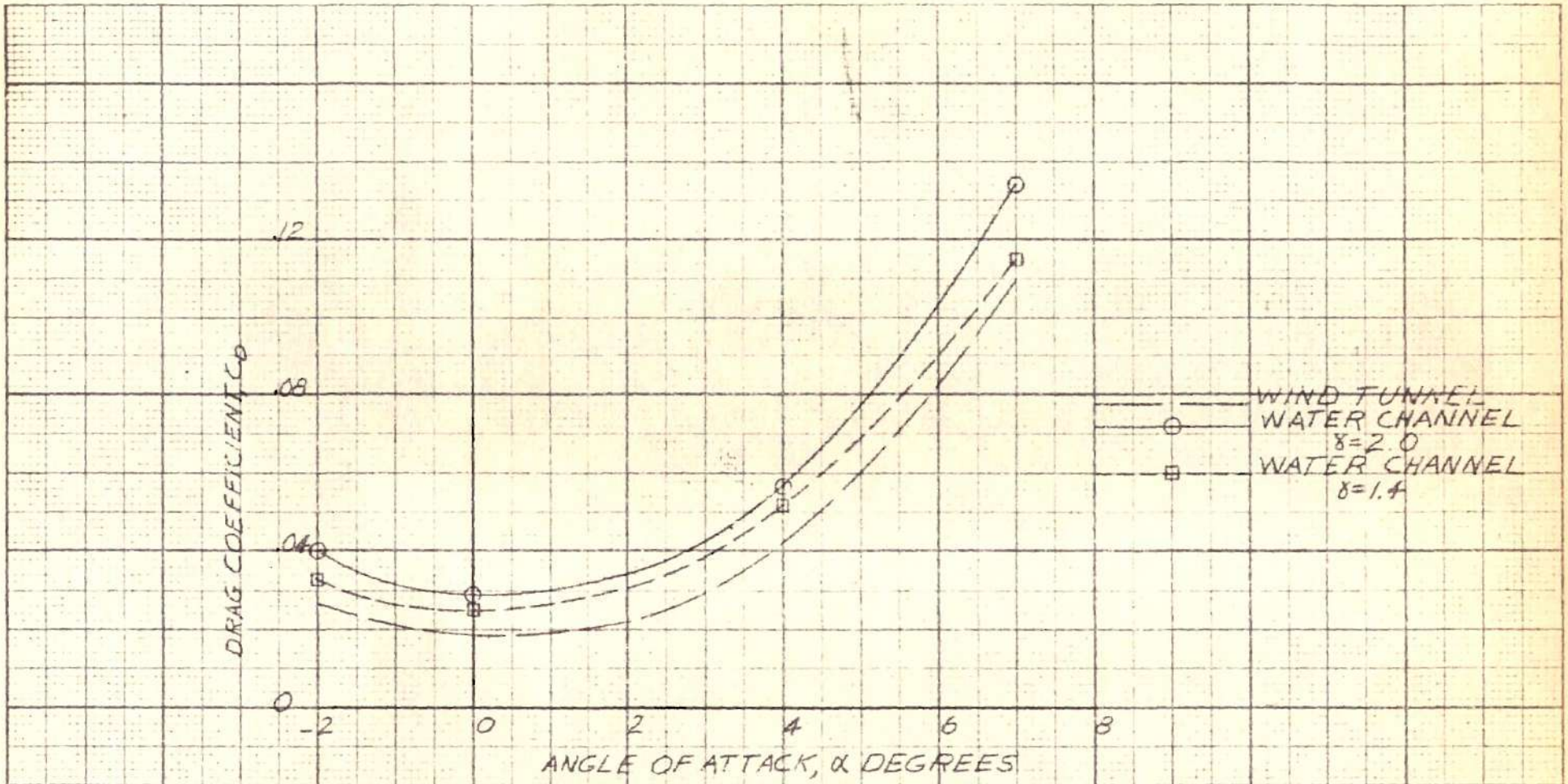

FIGURE 22. DRAG CURVES FOR FAIRED DOUBLE WEDGE AIRFOIL AT M=.8

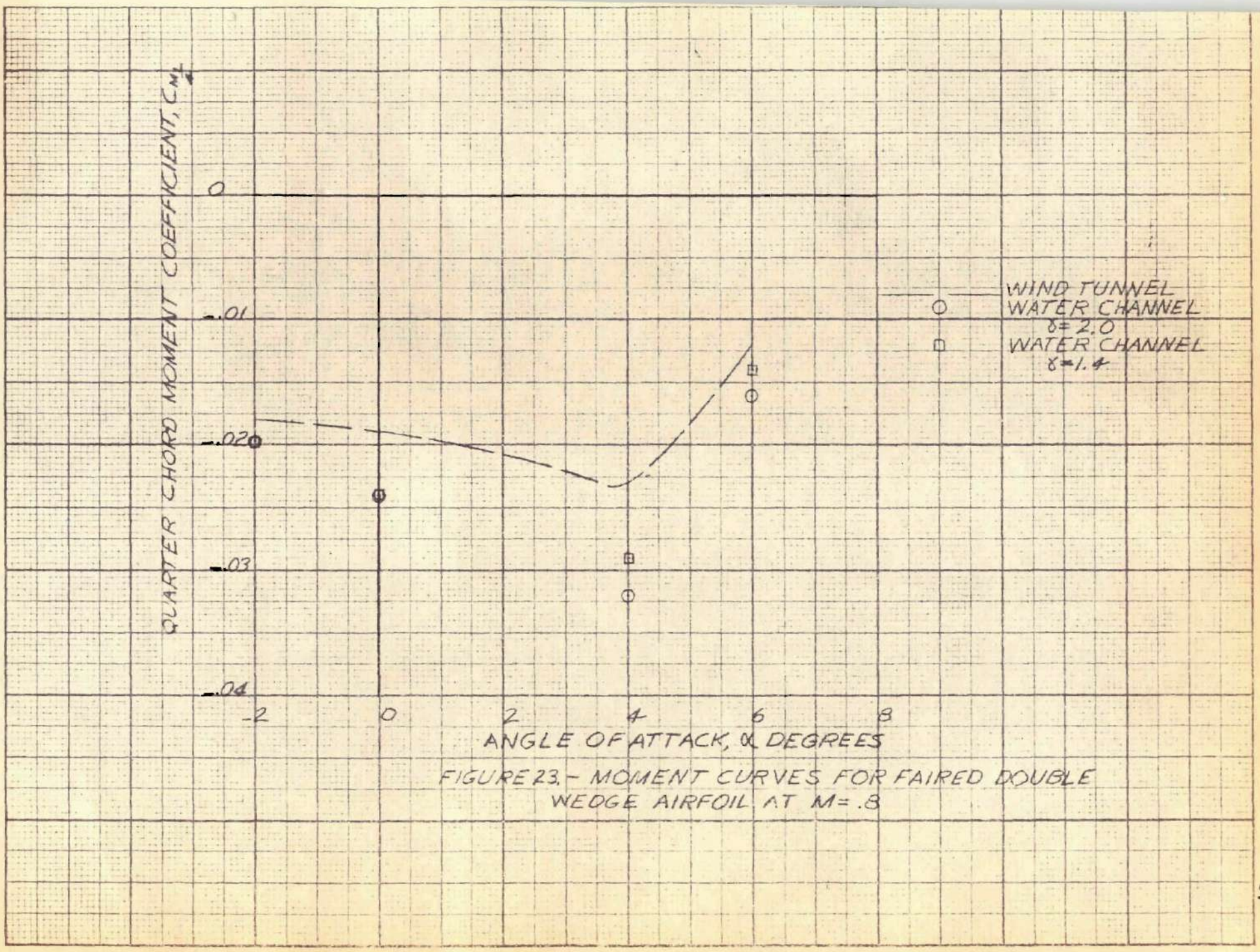

FIGURE 23.- MOMENT CURVES FOR FAIRED DOUBLE WEDGE AIRFOIL AT M = .8

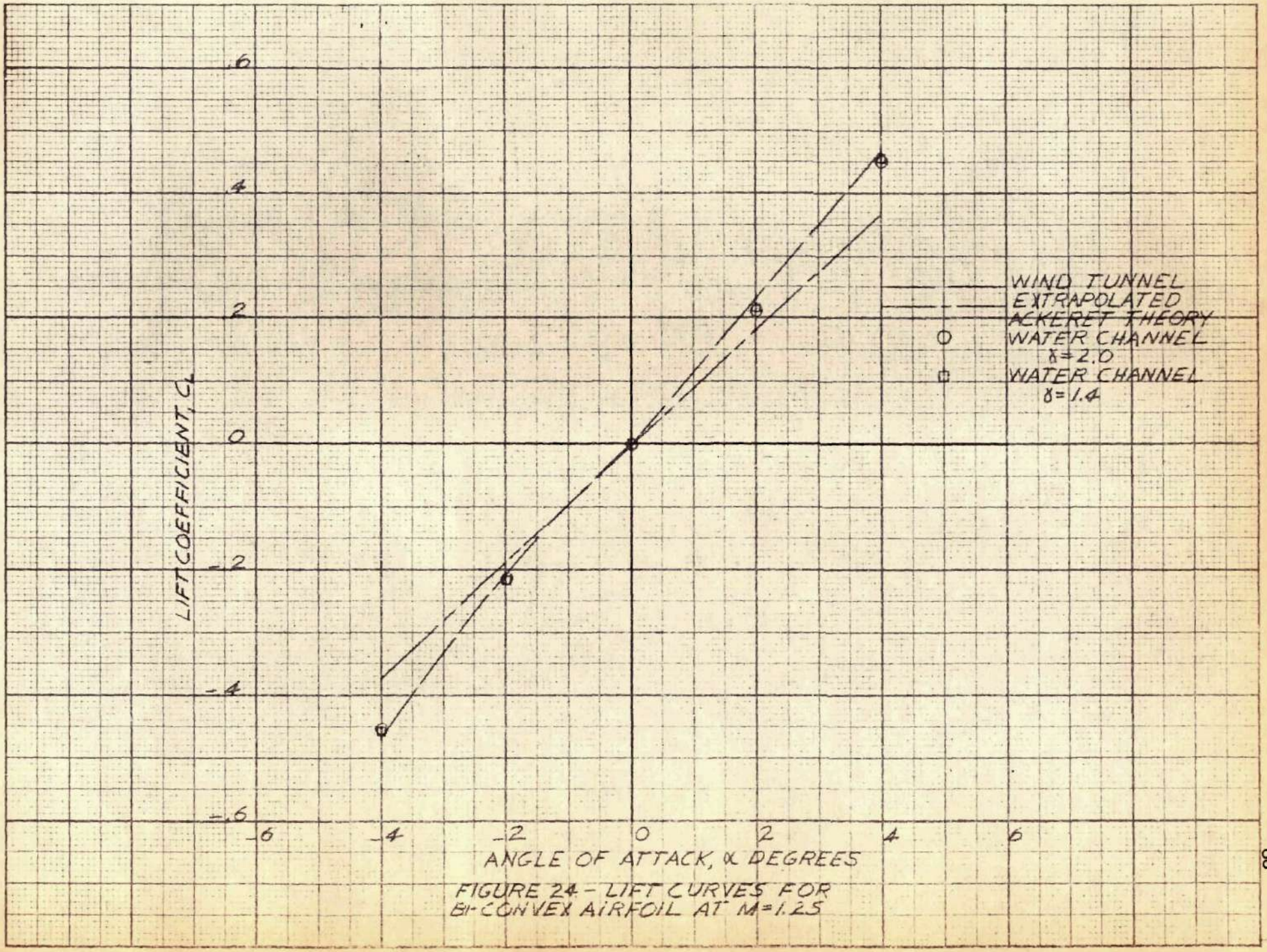

FIGURE 24 - LIFT CURVES FOR BI-CONVEX AIRFOIL AT M=1.25

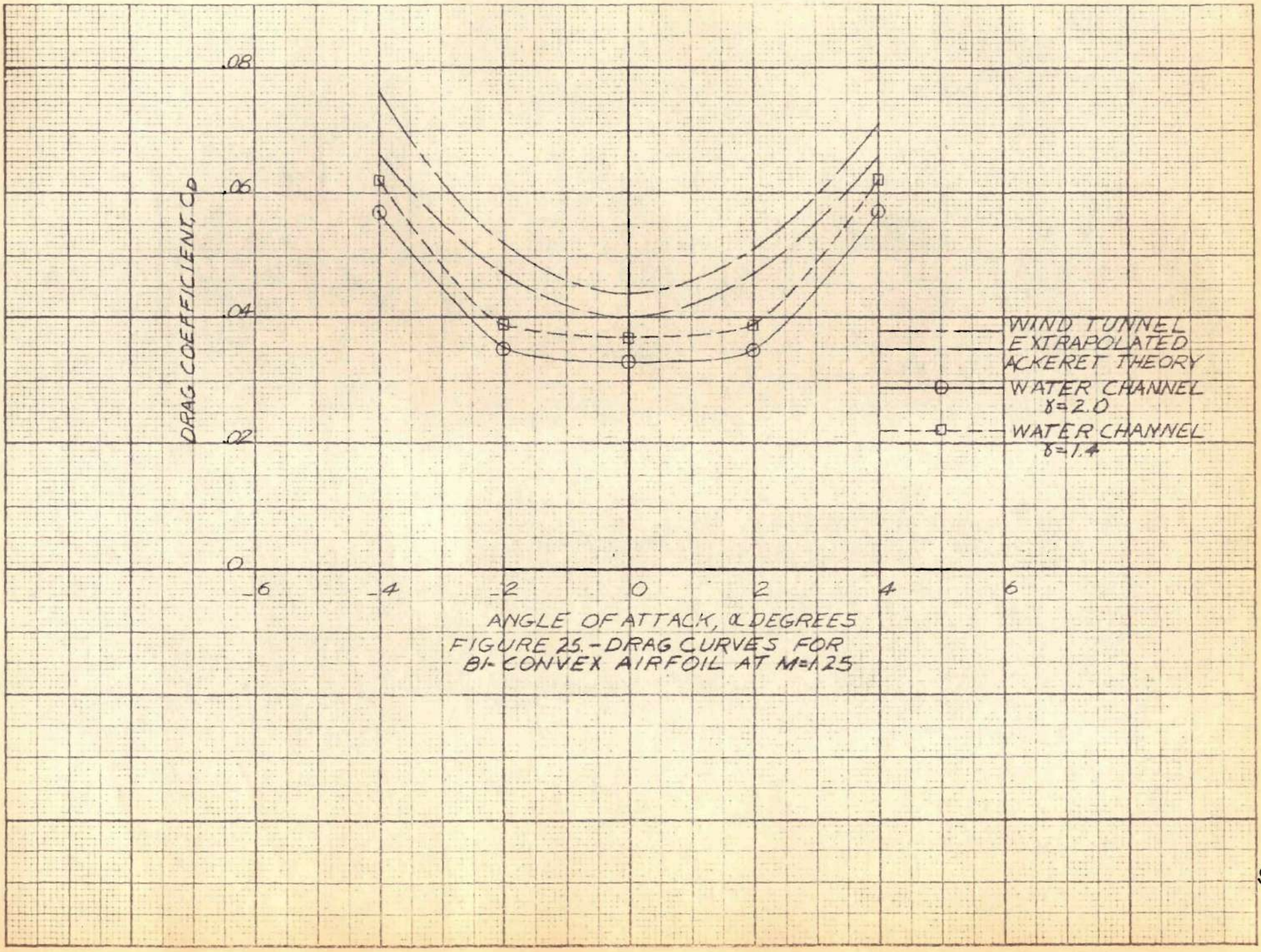

FIGURE 25. - DRAG CURVES FOR BI-CONVEX AIRFOIL AT M=1.25

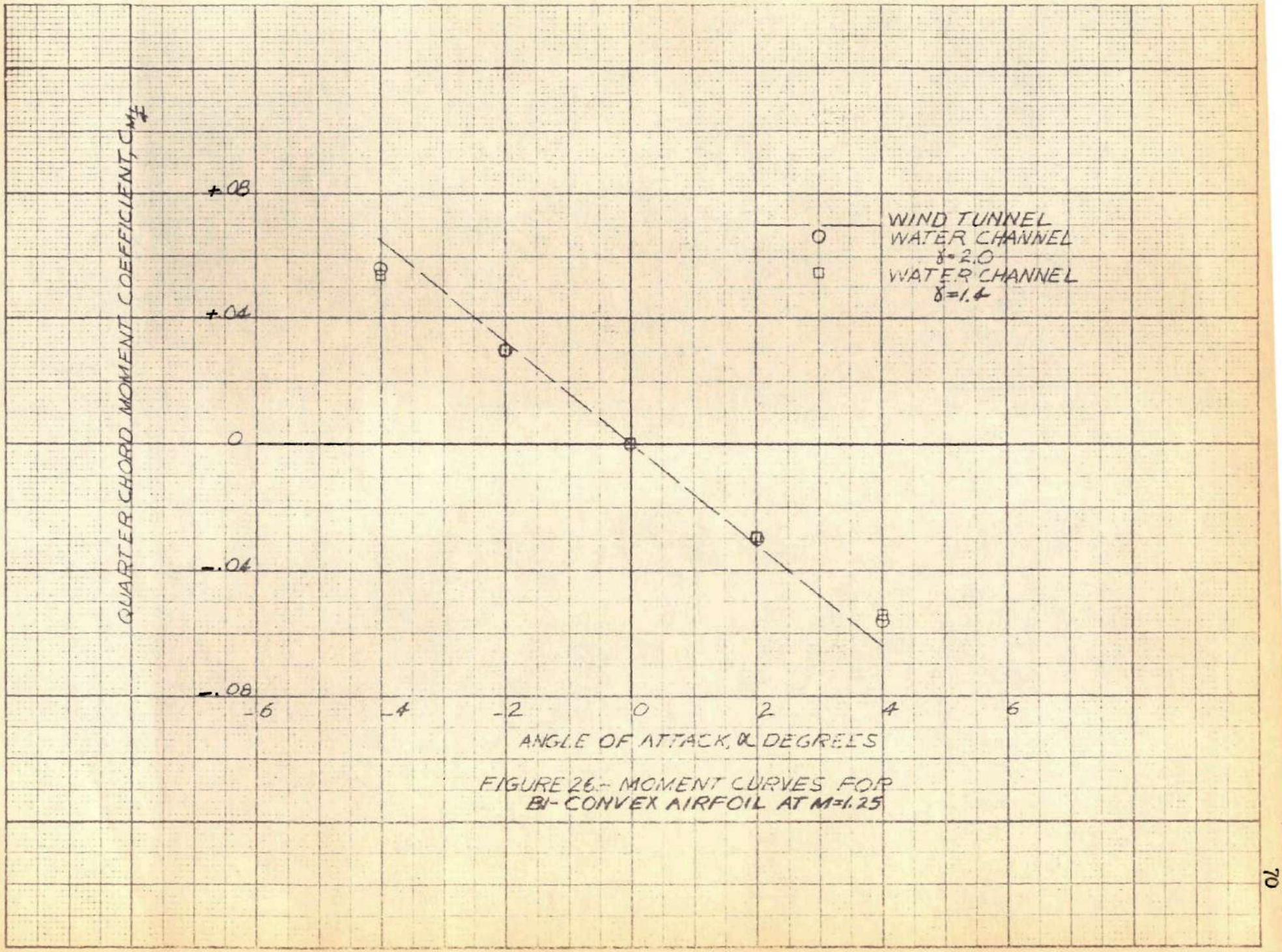

FIGURE 26.- MOMENT CURVES FOR BI-CONVEX AIRFOIL AT M=1.25

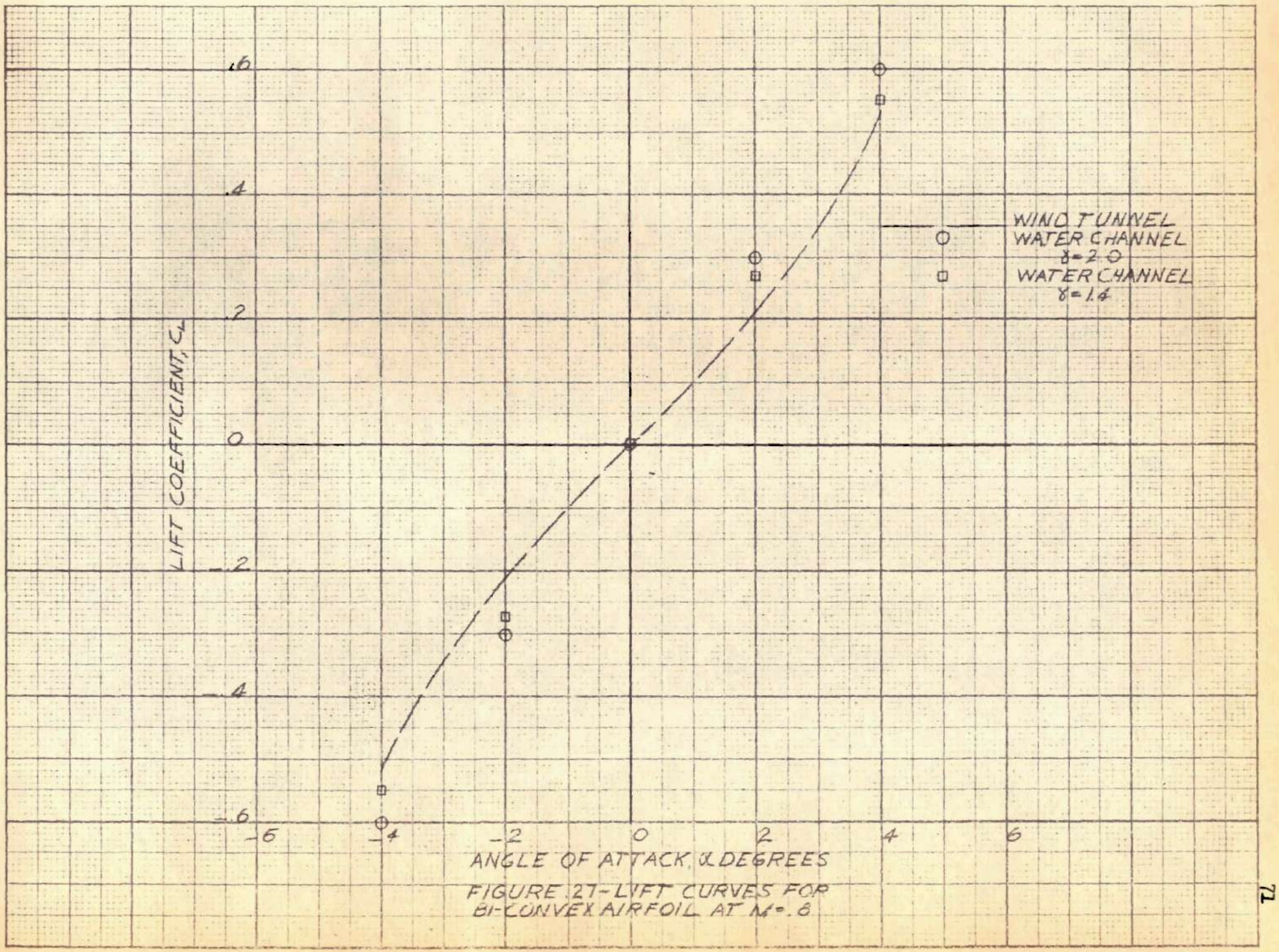

FIGURE 27-LIFT CURVES FOR BI-CONVEX AIRFOIL AT M=.6

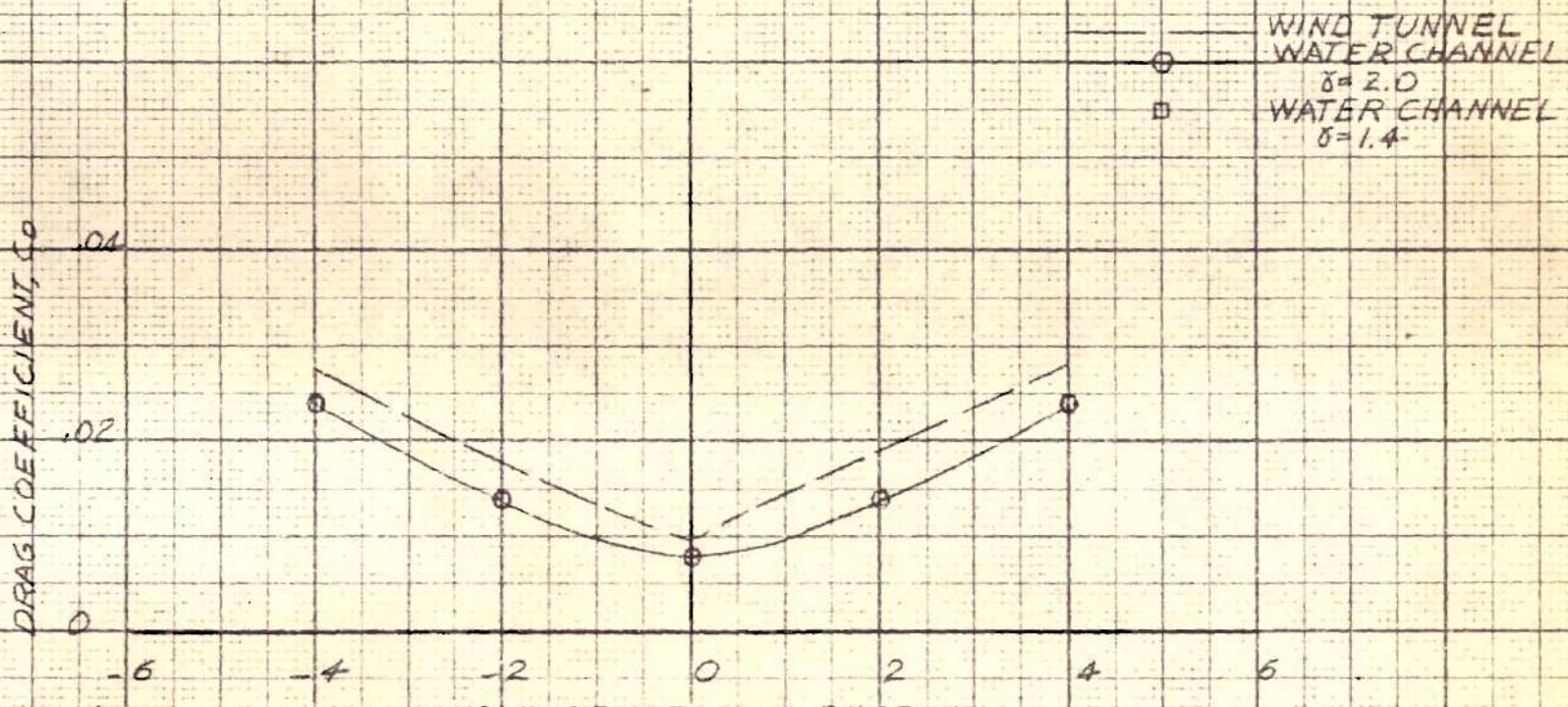

FIGURE 23 - DRAG CURVES FOR BI-CONVEX AIRFOIL AT M=.8

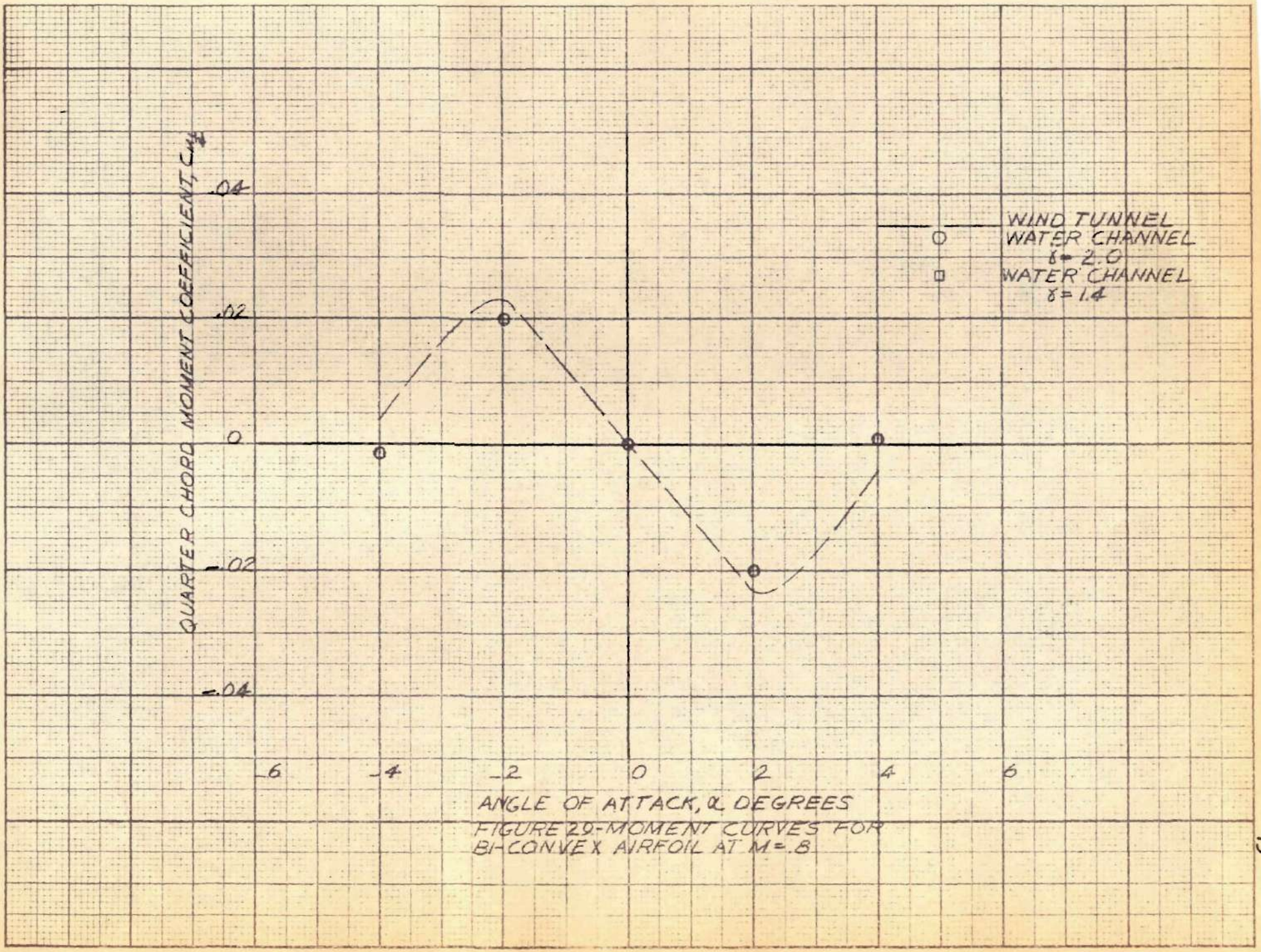

FIGURE 29-MOMENT CURVES FOR BI-CONVEX AIRFOIL AT M=.8

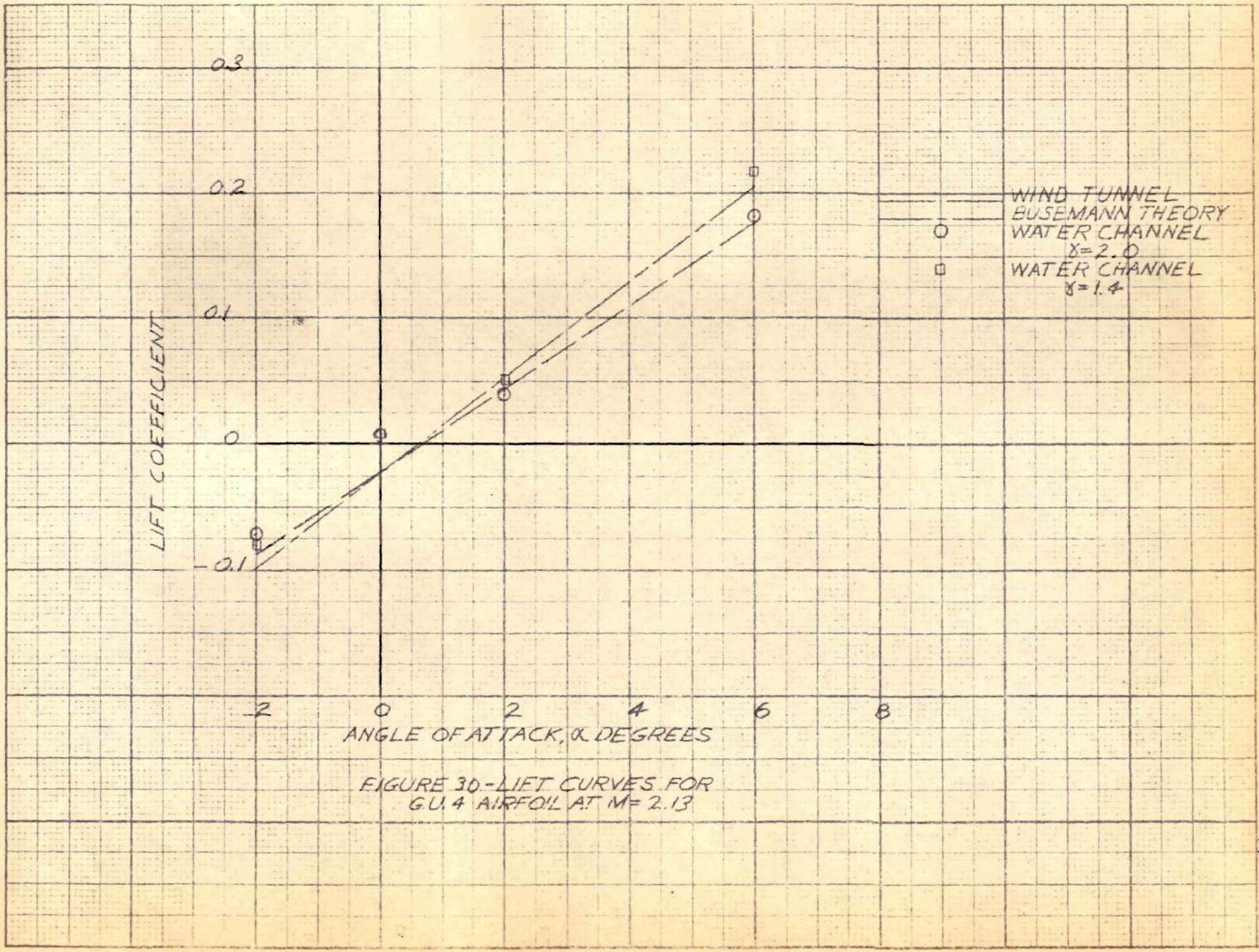

FIGURE 30 - LIFT CURVES FOR G.U.4 AIRFOIL AT M=2.13

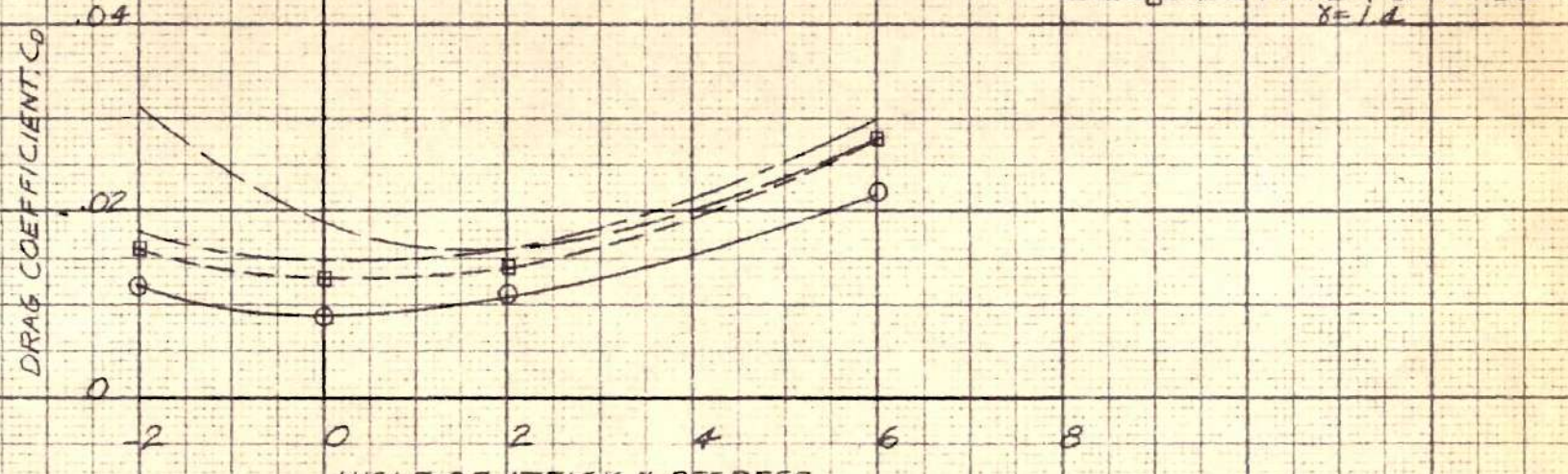

FIGURE 31- DRAG CURVES FOR G.U.4 AIRFOIL AT M= 2.13

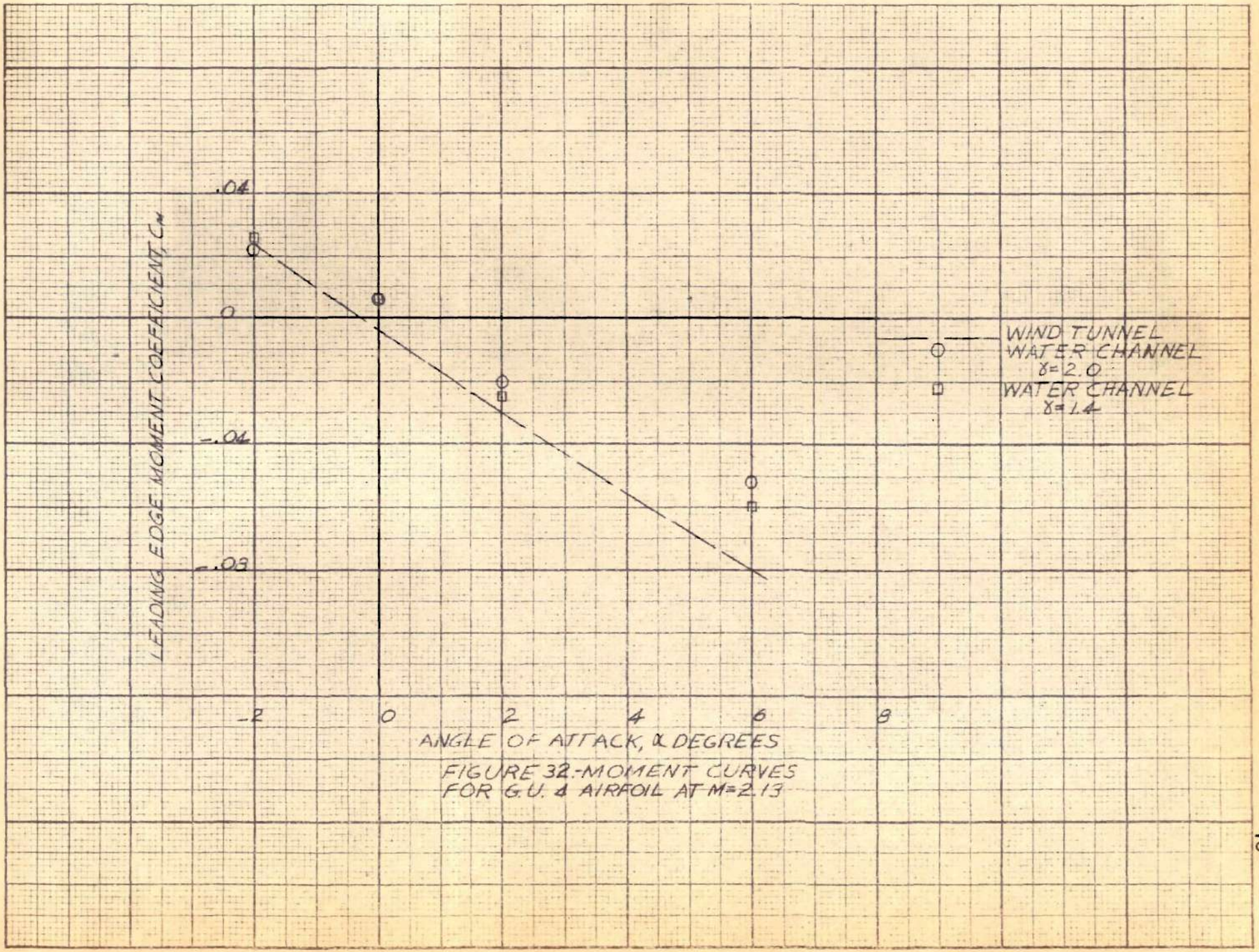

FIGURE 32.-MOMENT CURVES FOR G.U. 4 AIRFOIL AT M=2.13

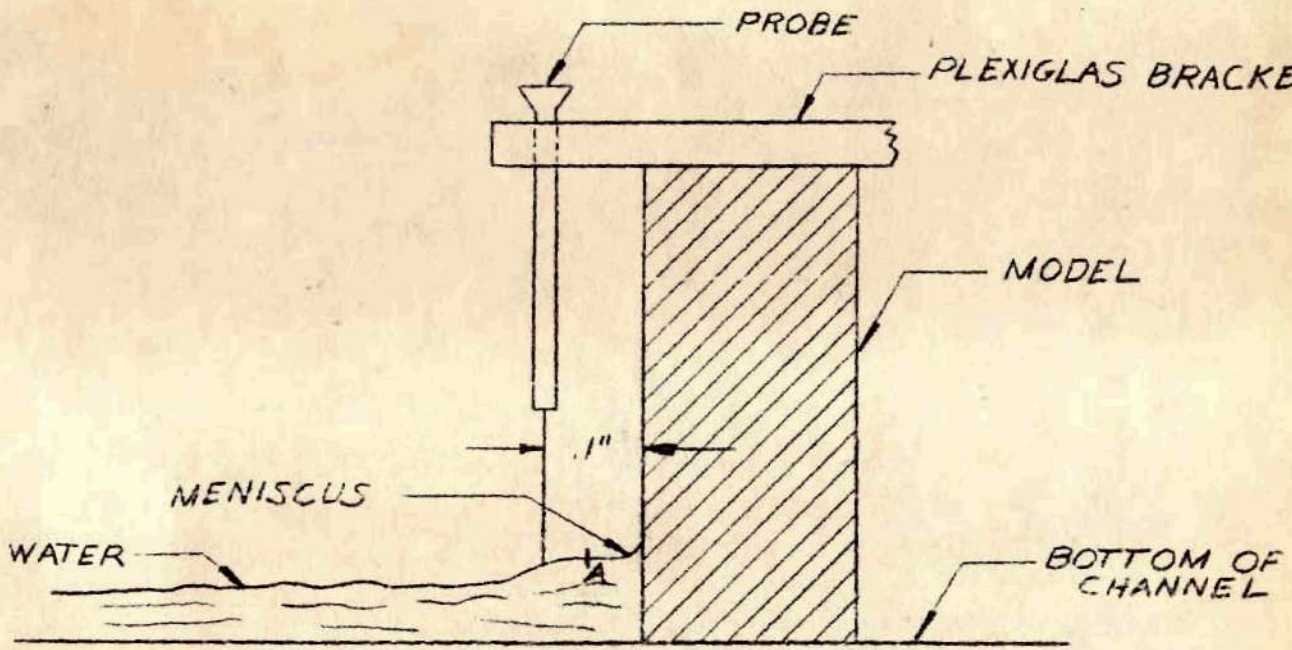

FIGURE 33-SCHEMATIC VIEW OF PROBE POSITION